(NAc) (Koob 1992; Wise 1996; Koob *et al.* 1998). The principal target for the action of METH is believed to be the dopamine transporter (DAT), which is a member of the solute carrier 6 (SLC6) gene family of Na^+/Cl^- coupled transporters that also includes the neurotransmitter transporters of norepinephrine, serotonin, glycine, and γ-aminobutyric acid (GABA) (Amara and Kuhar 1993; Torres *et al.* 2003; Chen *et al.* 2004). The DAT controls dopaminergic signaling by the rapid reuptake of dopamine (DA) from synaptic clefts. As a substrate, METH not only competitively inhibits DA uptake and thereby increases synaptic DA but also promotes the reverse transport of nonvesicular DA, resulting in an efflux of DA via the DAT (Sulzer *et al.* 2005; Fog *et al.* 2006). This efflux results in a dramatic increase in extracellular DA and is believed to be of major importance for the psychostimulant properties of METH (Sulzer *et al.* 2005; Fog *et al.* 2006). However, the exact neuronal circuits and molecular cascade essential for drug dependence are still poorly understood. Moreover, the molecules related to the METH-induced increase in DA efflux are unclear.

Tumor necrosis factor-α (TNF-α) plays an important role in a variety of infectious, inflammatory, and autoimmune conditions (Vassalli 1992). TNF-α also affects the CNS directly or indirectly through the stimulation of vagal afferents (Maier and Watkins 1998). Thus, this proinflammatory cytokine is emerging as a modulator of CNS function. Recently, we have demonstrated that TNF-α activates synaptosomal and vesicular DA uptake (Nakajima *et al.* 2004). Moreover, we have reported that TNF-α and its inducer diminish METH and morphine-induced behavioral sensitization and rewarding effects by promoting plasmalemmal and vesicular DA uptake as well as attenuating the METH and morphine-induced increase in overflow of DA in the NAc (Nakajima *et al.* 2004; Niwa *et al.* 2007b,d; Niwa *et al.* 2008). TNF-α modulates cellular responses through the extracellular signal-regulated kinase 1/2 (ERK1/2) and nuclear factor-κB (NF-κB) signaling pathways (van Vliet *et al.* 2005). ERK1/2 regulates the surface expression and capacity of DAT (Morón *et al.* 2003). However, the mechanisms by which TNF-α regulates the uptake of DA are poorly understood.

Recently, we have identified a novel molecule 'shati' in the NAc of mice treated with METH repeatedly using the polymerase chain reaction (PCR)-select complementary DNA (cDNA) substraction method, which is a differential and epochal cloning technique. Further, we have demonstrated that shati, which contains the sequence of GCN5-related *N*-acetyltransferase (GNAT), acetyl-CoA-binding sites, and ATP-binding sites, is involved in METH-induced hyperlocomotion, sensitization, and conditioned place preference (Niwa *et al.* 2007a). Blockage of shati expression by shati antisense oligonucleotide (shati-AS) potentiates not only the increase in extracellular DA levels, but also the decrease in synaptosomal and vesicular DA uptake in the NAc induced by repeated METH treatment, resulting in potentiation of the METH-induced dependence (Niwa *et al.* 2007a).

Pheochromocytoma-12 (PC12) cells are useful as a model of the neuronal system and have DATs. In the present study, we investigated the effects of TNF-α on DA uptake in PC12 cells and the involvement of the mitogen-activated protein kinase kinase (MEK) pathway in the effects of TNF-α on DA uptake. Moreover, we succeeded in the transfection of a vector containing shati cDNA into PC12 cells, investigated the involvement of shati in DA uptake and the METH-induced decrease in DA uptake, and examined the relationship between shati and TNF-α by using these PC12 cells.

Materials and methods

Cell culture and transfection

PC12 cells purchased from the Riken cell bank (No. RCB0009) were cultured on poly-ornithine-coated coverslips in Dulbecco's modified Eagle's medium (Sigma-Aldrich St Louis, MO, USA) supplemented with 10% heat inactivated horse serum and 5% fetal bovine serum (Loder and Melikian 2003). We made the vector containing shati cDNA with the suggested sequence of NM_001001985 using the plasmid pcDNA-DEST53 (Invitrogen, Carlsbad, CA, USA) as an expression vector with green fluorescent protein (GFP), although N-terminal of seven amino acids of shati was missing (CDS 882-1760) in this vector. For transient expression, the cells were transfected with the plasmid expressing shati using Lipofectamine 2000 (Invitrogen).

[^{3}H] DA uptake in PC12 cells

The uptake of [^{3}H] DA in PC12 cells was performed as described before (Melikian and Buckley 1999). The cells were washed in Krebs-Ringers- 4-(2-hydroxyethyl)-1-piperazineethanesulfonic acid buffer twice before the assay. Uptake was initiated by adding 1 μM [^{3}H] DA (Perkin Elmer, Waltham, MA, USA) containing 10^{-5} M pargyline and 10^{-5} M ascorbic acid. Uptake proceeded for 10 min at 23°C and was terminated with three rapid washes in ice-cold Krebs-Ringers-4-(2-hydroxyethyl)-1-piperazineethanesulfonic acid buffer. The amount of [^{3}H] DA accumulated was determined by liquid scintillation counting (Beckman Coulter, Inc., Fullerton, CA, USA). Non-specific uptake was defined in the presence of 10 μM [1-(2[bis(4-fluorophenyl-) methoxy]ethyl)-4-(3-phenylpropyl)piperazine] bimesylate hydrate (GBR 12909). The cells were pre-treated with TNF-α (0.1, 1, and 10 ng/mL) for 40 min, and assayed for [^{3}H] DA uptake. To neutralize TNF-α in PC12 cells, the cells were pre-treated with polyclonal goat anti-TNF-α antibody (R&D Systems Ltd., Minneapolis, MN, USA; Ab; 1, 10, 50, and 100 ng/mL) or soluble TNF receptor I (R&D Systems Ltd, sRI; 0.1, 0.5, 1, and 10 ng/mL) 10 min before the treatment with TNF-α (10 ng/mL, 40 min) (Barone *et al.* 1997), and assayed for [^{3}H] DA uptake. The function of TNF-α is mediated through two distinct cell surface receptors, TNF receptor I and TNF receptor II. The majority of TNF functions are mediated primarily through TNF receptor I, whereas TNF receptor II seems to play a role in only a limited number of

TNF responses (Hsu *et al.* 1995). Moreover, it has been reported that immunoreactivity for TNF receptor I is found in cell bodies and process of dopaminergic neurons (Boka *et al.* 1994). Therefore, we have used soluble TNF receptor I for neutralization for TNF-α. To examine the involvement of the MEK pathway in the TNF-α-induced increase in DA uptake in PC12 cells, the cells were pre-treated with a selective MEK inhibitor 2-(2-amino-3-methyoxy-phenyl)-4H-1-benzopyran-4-one (Calbiochem, San Diego, CA, USA; PD98059; 1, 10, 100, and 500 μM) 10 min before their treatment with TNF-α (10 ng/mL, 40 min), and assayed for [^{3}H] DA uptake. PD98059 was dissolved in dimethyl sulfoxide to give a concentration of 50 mM, stored in aliquots at −80°C, and diluted in Dulbecco's modified Eagle's medium to 1–500 μM immediately prior to use. To examine the effects of TNF-α on the METH-induced decrease in DA uptake in PC12 cells, the cells were pre-treated with TNF-α (10 ng/mL) 10 min before being treated with METH (1 μM, 30 min), and assayed for [^{3}H] DA uptake, following previous observations (Nakajima *et al.* 2004). Cen *et al.* (2008) have reported that METH (1 μM) decreases plasmmalemmal DAT expression in time-dependent manner (0, 5, 15, 30, 60 min), which is paralleled with the decrease in [^{3}H] DA uptake. Since treatment of METH (1 μM) for 30 min significantly decreases DA uptake compared with control group (Cen *et al.*, 2008), we have selected this time point for treatment of METH before the uptake assay. To examine the involvement of TNF-α in the shati-induced increase in [^{3}H] DA uptake in the shati-over-expressing PC12 cells, the cells were pre-treated with polyclonal goat anti-TNF-α antibody (R&D Systems Ltd, Ab; 50 ng/mL) or soluble TNF receptor I (R&D Systems Ltd, sR I; 1 ng/mL) 10 min before their treatment with METH (1 μM, 30 min), and assayed for [^{3}H] DA uptake.

Immunocytochemistry

Two antibodies against the peptide of the hypothetical protein, CNTAFRGLRQHPRTQLL (S-3) and CMSVDSRFRGKGIAKALG (S-4) unique to shati were generated. These peptides were conjugated to keyhole limpet hemocyanin and injected into rabbits six times at 1-week intervals. Serum was taken from the rabbits 1 week after the final injection. The serum was diluted 200 times for immunostaining (Niwa *et al.* 2007a).

Transfected PC12 cells attached to glass coverslips were fixed with 4% paraformaldehyde in phosphate-buffered saline for 20 min, and then blocked in 3% normal sera and 0.1% Triton X-100 for 1 h. The coverslips were incubated with primary antibodies at 4°C overnight, washed with phosphate-buffered saline, and then incubated with appropriate secondary antibodies for 2 h. Polyclonal rabbit anti-S-3 or anti-S-4 antibody (1 : 200), monoclonal mouse anti-tyrosine hydroxylase (TH) antibody (1 : 200, Chemicon, Temecula, CA, USA), monoclonal mouse anti-GFP antibody (1 : 500, Chemicon), polyclonal goat anti-rat TNF-α antibody (1 : 100, R&D Systems Ltd), and polyclonal rabbit anti-GFP antibody (1 : 100, Chemicon) served as primary antibodies. Goat anti-mouse Alexa Fluor 546 (1 : 1000, Invitrogen), donkey anti-goat Alexa Fluor 546 (1 : 1000, Invitrogen), rabbit anti-mouse Alexa Fluor 488 (1 : 1000, Invitrogen), and donkey anti-rabbit Alexa Fluor 488 (1 : 1000, Invitrogen) were used as secondary antibodies. After being washed and mounted, stained cells were observed under a fluorescence microscope (Axioskoop 2 plus). Because similar results were obtained using the anti S-3 and anti-S-4 antibodies in the immunohistochemical experiments, only the data obtained with the anti-S-4 antibody is described.

Real time reverse transcription-polymerase chain reaction

Total RNA was isolated using an RNeasy Kit (Qiagen, Hilden, Germany) and converted into cDNA using a SuperScript™ First-Strand System for RT-PCR Kit (Invitrogen). The levels of shati and TNF-α mRNA were determined by real-time RT-PCR using a TaqMan probe. The 18S ribosomal RNA was used as the internal control (Applied Biosystems, CA, USA). The shati primers used for real-time RT-PCR were as follows: 5′-TGTAAACACCCCTAA AGTGCCCT-3′ (forward; bp 2967–2989) and 5′-TCAATCCTGC ATACAAGGAATCAA-3′ (reverse; bp 3022–3045), and the Taq-Man probe was 5′-CACAGTCTGTGAGGCTCAGGTTGCCC-3′ (probe; bp 2995–3020). The amplification consisted of an initial step (95°C for 5 min) and then 40 cycles of denaturation for 30 sec at 95°C, annealing for 40 s at 59°C, and the extension time for 1 min at 72°C in an iCycle iQ Detection System (Bio-Rad Laboratories, Inc., CA, USA) (Niwa *et al.* 2007a). The expression levels were calculated as described previously (Wada *et al.* 2000).

Animals

The male C57BL/6J- wild-type mice were obtained from Slc Japan (Hamamatsu, Japan). Animals were housed in plastic cages and kept in a temperature-, humidity-, and light-controlled room (23 ± 1°C; 50 ± 5% humidity; 12 : 12 h light/dark cycle starting at 8:00 AM) and had free access to food and water, except during behavioral experiments. All animal care and use was in accordance with the National Institutes of Health Guide for the Care and Use of Laboratory Animals and approved by the Institutional Animal Care and Use Committee of Nagoya University School of Medicine. Animals were treated according to the Guidelines of Experimental Animal Care issued from the Japanese Pharmaceutical Society.

Shati-antisense oligonucleotide (shati-AS) treatment

Mice were anesthetized with pentobarbital (40 mg/kg, i.p.) and placed in a stereotaxic apparatus. The infusion cannula was connected to a miniosmotic pump (total capacity was 90 μL, Alzet 1002; Alza, Palo Alto, CA, USA) filled with shati-antisense oligonucleotide (shati-AS) or -scrambled oligonucleotide (shati-SC). The pump was implanted into the right ventricle [anteroposterior (AP) −0.5 mm, mediolateral +1.0 mm from the bregma, and dorsoventral −2.0 mm from the skull, according to the atlas of Franklin and Paxinos (1997)]. Phosphorothionate oligonucleotides were custom-synthesized at Nisshinbo Biotechnology (Tokyo, Japan) and dissolved in artificial CSF (147 mM NaCl, 3 mM KCl, 1.2 mM $CaCl_2$, and 1.0 mM $MgCl_2$, pH 7.2). The oligonucleotides were phosphorothioated at the first three bases of both the 5′- and 3′-ends, which results in increased stability and less toxicity. The sequences of shati-AS and -SC were 5′-TCTTCGTCTCGCAGAC CATGTCG-3′ and 5′-GGTCTGCTACACTGCTGCTAGTC-3′, respectively. Shati-AS and -SC were continuously infused into the cerebral ventricle at a dose of 1.8 nmol/6 μL/day (flow rate, 0.25 μL/h). Additionally, shati-SC was used as a control. Three days after the start of oligonucleotide infusion, mice were

administered METH (1 mg/kg, s.c.) for 5 days and decapitated 2 h after the final treatment (Niwa *et al.* 2007a).

Statistical analysis

All data were expressed as means ± SE. Statistical differences between two groups were determined with Student's *t*-test. Statistical differences among three groups or more were determined using a one-way analysis of variance (ANOVA), two-way ANOVA, or three-way ANOVA, followed by the Bonferroni multiple comparison test. $p < 0.05$ was regarded as statistically significant.

Nucleotide sequences

The DNA Data Bank of Japan/GenBank/European Molecular Biology Laboratory accession number for the primary nucleotide sequence of shati is DQ174094.

Results

Effect of TNF-α on DA uptake in PC12 cells

First, we investigated the effects of TNF on DA uptake in PC12 cells, since we have recently demonstrated that TNF-α activates synaptosomal and vesicular DA uptake in mice (Nakajima *et al.* 2004).

TNF-α (10 ng/mL, 40 min) increased [^{3}H] DA uptake compared with the control group ($F_{3,28} = 4.933$, $p < 0.01$, one-way ANOVA) (Fig. 1a). Moreover, we investigated whether the TNF-α-induced increase was antagonized by the anti-TNF-α antibody and soluble TNF receptor in PC12 cells. Pre-treatment with the antibody (10, 50, and 100 ng/

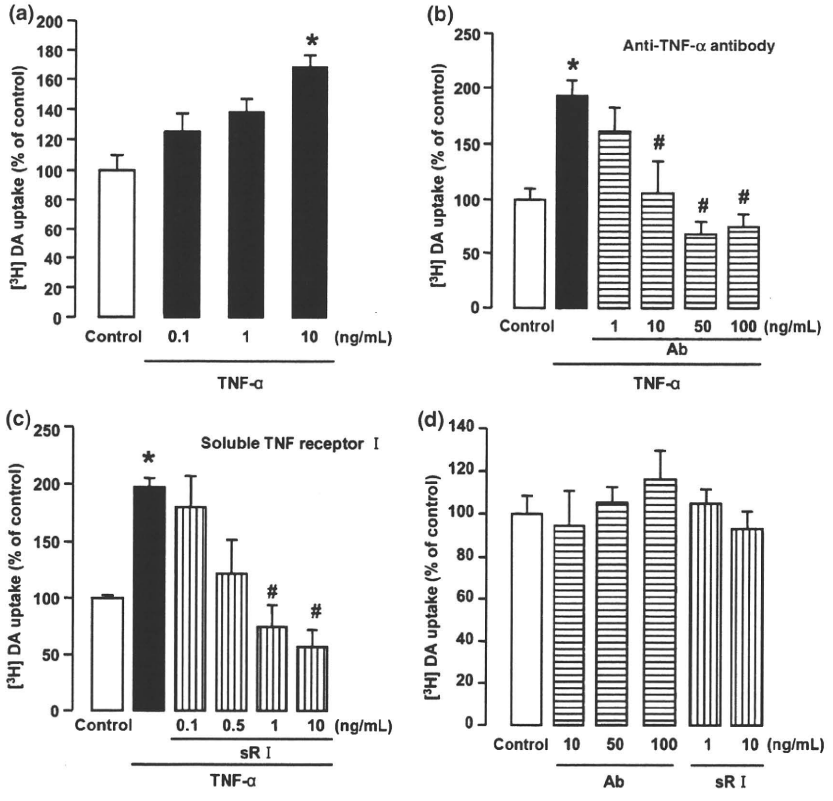

Fig. 1 Effects of anti-TNF-α antibody (Ab) or soluble TNF receptor I (sR I) on TNF-α-induced increase in [^{3}H] DA uptake in PC12 cells. (a) The cells were pre-treated with TNF-α (0.1, 1, and 10 ng/mL) for 40 min, and assayed for [^{3}H] DA uptake. The [^{3}H] DA uptake was 0.14 ± 0.01 pmol/10 min for control. The final concentration of [^{3}H] DA was 20 nM. Value are means ± SE ($n = 8$). *$p < 0.05$ versus control. (b) Effects of anti-TNF-α antibody (Ab) on TNF-α-induced increase in [^{3}H] DA uptake in PC12 cells. The cells were pre-treated with anti-TNF-α antibody (1, 10, 50, and 100 ng/mL) 10 min before their treatment with TNF-α (10 ng/mL, 40 min), and assayed for [^{3}H] DA uptake. The [^{3}H] DA uptake was 0.10 ± 0.02 pmol/10 min for the control. The final concentration of [^{3}H] DA was 20 nM. Values are means ± SE ($n = 6$–7). *$p < 0.05$ versus control. $^{\#}p < 0.05$ versus TNF-α-treated cells. (c) Effects of soluble TNF receptor I (sR I) on TNF-α-induced increase in [^{3}H] DA uptake in PC12 cells. The cells were pre-treated with soluble TNF receptor I (0.1, 0.5, 1, and 10 ng/mL) 10 min before being treated with TNF-α (10 ng/mL, 40 min), and assayed for [^{3}H] DA uptake. The [^{3}H] DA uptake was 0.06 ± 0.00 pmol/10 min for the control. The final concentration of [^{3}H] DA was 20 nM. Values are means ± SE ($n = 6$–7). *$p < 0.05$ versus control. $^{\#}p < 0.05$ versus TNF-α-treated cells. (d) Effects of anti-TNF-α antibody (Ab) or soluble TNF receptor I (sR I) on [^{3}H] DA uptake in PC12 cells. The cells were pre-treated with anti-TNF-α antibody (10, 50, and 100 ng/mL) or soluble TNF receptor I (1 and 10 ng/mL) for 50 min, and assayed for [^{3}H] DA uptake. The [^{3}H] DA uptake was 0.08 ± 0.01 pmol/10 min for the control. The final concentration of [^{3}H] DA was 20 nM. Values are means ± SE ($n = 6$–8).

mL, 50 min) or soluble TNF receptor I (1 and 10 ng/mL, 50 min) significantly inhibited the TNF-α-induced increase in [^{3}H] DA uptake ($F_{5,34}$ = 7.370 for anti-TNF-α antibody; $F_{5,34}$ = 7.526 for soluble TNF receptor I, $p < 0.01$, one-way ANOVA) (Fig. 1b and c), although the anti-TNF-α antibody (10, 50, and 100 ng/mL, 50 min) or soluble TNF receptor I (1 and 10 ng/mL, 50 min) itself had no effect on DA uptake (Fig. 1d). These results suggest that TNF-α activates DA uptake in PC12 cells.

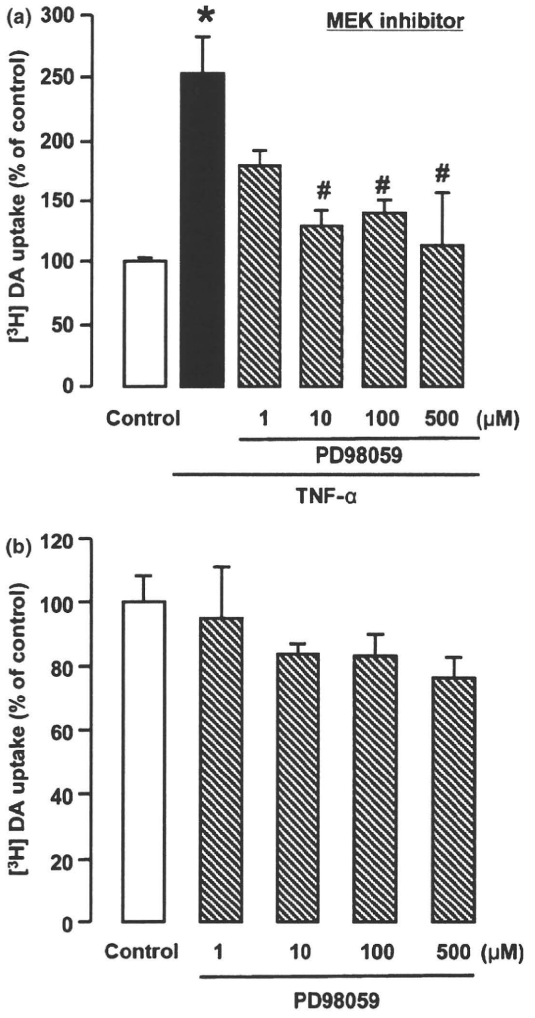

Fig. 2 Effects of MEK inhibitor on TNF-α-induced increase in [^{3}H] DA uptake in PC12 cells. (a) Effects of the MEK inhibitor PD98059 on TNF-α-induced increase in [^{3}H] DA uptake in PC12 cells. The cells were pre-treated with PD98059 (1, 10, 100, and 500 μM) 10 min before their treatment with TNF-α (10 ng/mL, 40 min), and assayed for [^{3}H] DA uptake. The [^{3}H] DA uptake was 0.10 ± 0.00 pmol/10 min for control. The final concentration of [^{3}H] DA was 20 nM. Values are means ± SE (n = 4). *$p < 0.05$ versus control. #$p < 0.05$ versus TNF-α-treated cells. (b) Effects of PD98059 on [^{3}H] DA uptake in PC12 cells. The cells were pre-treated with PD98059 (1, 10, 100, and 500 μM) for 50 min, and assayed for [^{3}H] DA uptake. The [^{3}H] DA uptake was 0.12 ± 0.00 pmol/10 min for the control. The final concentration of [^{3}H] DA was 20 nM. Values are means ± SE (n = 4).

Effects of mitogen-activated protein kinase kinase inhibitor on TNF-α-induced increase in DA uptake in PC12 cells

TNF-α modulates cellular responses through the ERK1/2 signaling pathway (van Vliet *et al.* 2005). Therefore, we investigated whether the TNF-α-induced increase in DA

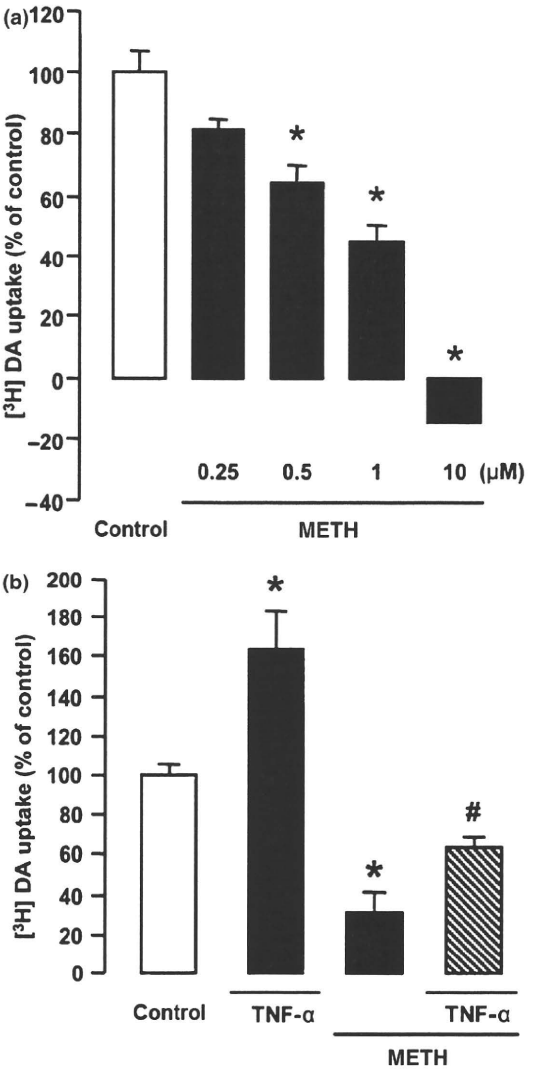

Fig. 3 Effects of TNF-α on METH-induced decrease in [^{3}H] DA uptake in PC12 cells. (a) Dose-response effects of METH on [^{3}H] DA uptake in PC12 cells. The cells were pre-treated with METH (0.25, 0.5, 1, and 10 μM) for 30 min, and assayed for [^{3}H] DA uptake. The [^{3}H] DA uptake was 0.28 ± 0.02 pmol/10 min for the control. The final concentration of [^{3}H] DA was 20 nM. Values are means ± SE (n = 4). *$p < 0.05$ versus control. (b) Effects of TNF-α on METH-induced decrease in [^{3}H] DA uptake in PC12 cells. The cells were pre-treated with TNF-α (10 ng/mL) 10 min before being treated with METH (1 μM, 30 min), and assayed for [^{3}H] DA uptake. The [^{3}H] DA uptake was 0.19 ± 0.01 pmol/10 min for the control. The final concentration of [^{3}H] DA was 20 nM. Values are means ± SE (n = 5). *$p < 0.05$ versus control. #$p < 0.05$ versus METH-treated cells.

uptake was antagonized by the MEK inhibitor PD98059 in PC12 cells.

Pre-treatment with PD98059 (10, 100, and 500 μM, 50 min) significantly inhibited the TNF-α-induced increase in [^{3}H] DA uptake ($F_{5,18} = 5.961$, $p < 0.01$, one-way ANOVA) (Fig. 2a), although PD98059 (1, 10, 100, and 500 μM, 50 min) itself had no effect on the uptake (Fig. 2b). These results suggest that TNF-α activates DA uptake via the MEK signaling pathway in PC12 cells.

Effects of TNF-α on METH-induced decrease in DA uptake in PC12 cells

We have previously demonstrated that TNF-α and its inducer diminish the METH-induced decrease in DA uptake and inhibit the rewarding effects of and sensitization to METH (Nakajima *et al.* 2004; Niwa *et al.* 2007c, e). Therefore, we confirmed the effects of TNF-α on the METH-induced decrease in DA uptake in PC12 cells.

METH (0.5, 1, and 10 μM, 30 min) decreased [^{3}H] DA uptake compared with the control group in a dose-dependent manner ($F_{4,15} = 83.675$, $p < 0.01$, one-way ANOVA) (Fig. 3a). Moreover, TNF-α (10 ng/mL, 40 min) inhibited the METH-induced decrease in [^{3}H] DA uptake (TNF-α, $F_{1,16} = 14.759$, $p < 0.01$; METH, $F_{1,16} = 45.994$, $p < 0.01$; TNF-α·METH $F_{1,16} = 1.573$, $p = 0.228$; two-way ANOVA) (Fig. 3b). These results suggest that TNF-α inhibits the METH-induced decrease in DA uptake in PC12 cells (Fig. 3) as well as promoting plasmalemmal and vesicular DA uptake to diminish METH and morphine-induced behavioral sensitization and rewarding effects (Nakajima *et al.* 2004; Niwa *et al.* 2007b; Niwa *et al.* 2008).

Transfection of the vector containing shati cDNA into PC12 cells

We established a PC12 cell line transfected with the vector containing shati cDNA to examine the role of shati in DA uptake and the METH-induced decrease in DA uptake.

We used immunostaining for TH to check morphological changes of the PC12 cells after the transfection of the vector containing shati cDNA. Morphological changes to the cells were not observed after the transfection compared with mock-transfected or non-transfected PC12 cells (Fig. 4a). To confirm the transfection of the vector containing shati cDNA, we checked for immunostaining against S-4 and GFP, co-expressed with shati. No immunoreactivity for S-4 or GFP was found in the cells that were mock-transfected, which express neither shati nor GFP [Fig. 4b (i)]. The cells mock-transfected (=expression vector [pcDNA-DEST53]), which express GFP, but not shati, were immunopositive for GFP, but not S-4 [Fig. 4b (ii)]. The cells transfected with the vector containing shati cDNA, which express both shati and GFP, were immunopositive for S-4 and GFP [Fig. 4b (iii)]. The cells immunopositive for S-4 were merged with those positive for GFP. These results indicated that shati was certainly expressed in PC12 cells and transfection did not affect cell survival or morphology.

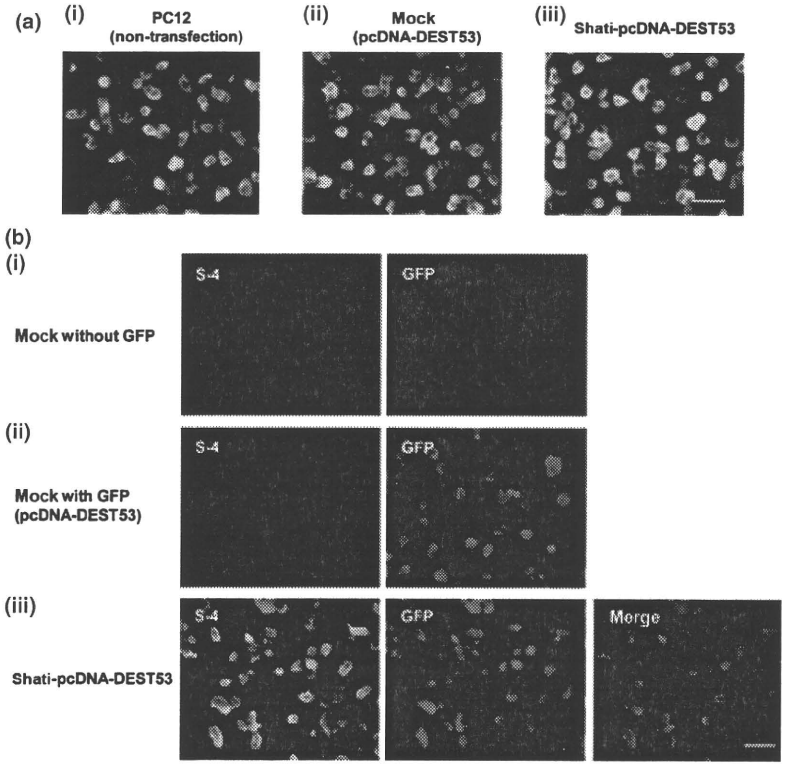

Fig. 4 Transfection of the vector containing shati cDNA into PC12 cells. (a) The morphological changes of the PC12 cells after transfection of the expression vector (pcDNA-DEST53) (ii) or vector containing shati cDNA (iii). The expression vector alone (mock-transfection) (ii), or the vector containing shati cDNA (iii) was introduced into PC12 cells. There were no changes in survival or morphology in the transfected PC12 cells. Scale bar: 20 μm. (b) Immunostaining of shati in PC12 cells transfected with the vector containing shati cDNA. pENTR/TEV/D-TOPO (without shati recombination and green fluorescent protein (GFP) site) (i), pcDNA-DEST53 with GFP (mock-transfection) (ii), or the vector containing shati cDNA and GFP (iii), was introduced into PC12 cells. The shati-immunopositive cells (green) were colocalized with GFP-immunopositive cells (red). Double immunostaining for S-4 and GFP in PC12 cells transfected with the vector containing shati cDNA reveals overexpression of shati in PC12 cells (iii). Scale bar: 20 μm.

Effect of over-expressed shati on DA uptake in PC12 cells

We have previously demonstrated that shati-AS, which inhibits the expression of shati mRNA, significantly potentiates the METH-induced decrease in synaptosomal and vesicular [^{3}H] DA uptake compared with that in the shati-SC or CSF-treated mice (Niwa *et al.* 2007a). Moreover, [^{3}H] DA uptake in saline-treated mice was also decreased by shati-AS compared with that in the CSF-treated mice, although shati-SC had no effect on [^{3}H] DA uptake (Niwa *et al.* 2007a). Given the results for synaptosomal and vesicular [^{3}H] DA uptake using shati-AS, we concluded that shati plays a critical role in modulating DA uptake. To address this issue, we investigated the role of shati in DA uptake in PC12 cells transfected with the vector containing shati cDNA.

Transfection of the vector containing shati cDNA increased shati mRNA expression compared with the mock-transfection, suggesting that shati was over-expressed in these cells (Fig. 5a left two columns). The increase in the levels of shati mRNA expression evoked by METH treatment (1 μM, 30 min) in mock-transfected cells was significantly potentiated by shati over-expression in PC12 cells (drug, $F_{1,28} = 20.917$, $p < 0.01$; transfection, $F_{1,28} = 247.684$, $p < 0.01$; drug × transfection, $F_{1,28} = 0.003$, $p = 0.955$; two-way ANOVA) (Fig. 5a right two columns).

We examined the *in vitro* effect of over-expressed shati on [^{3}H] DA uptake in PC12 cells. Shati-over-expressing cells themselves showed increased [^{3}H] DA uptake compared with the mock-transfected cells, suggesting that shati itself promotes DA uptake (Fig. 5b left two columns). We pre-treated PC12 cells with METH (1 μM) for 30 min, and then assayed the uptake of [^{3}H] DA. As shown in Fig. 5b, METH (1 μM, 30 min) decreased [^{3}H] DA uptake compared with the mock-transfected control cells. In the shati-over-expressing cells, the METH-induced decrease in [^{3}H] DA uptake was significantly inhibited compared with that in the mock-transfected cells (drug, $F_{1,40} = 45.807$, $p < 0.01$; transfection, $F_{1,28} = 21.551$, $p < 0.01$; drug × transfection, $F_{1,28} = 0.001$, $p = 0.971$; two-way ANOVA) (Fig. 5b right two columns). These results indicated that shati could attenuate METH-induced inhibition of DA uptake.

Regulation of TNF-α expression by shati

TNF-α activates synaptosomal and vesicular DA uptake (Nakajima *et al.* 2004). TNF-α and its inducer diminish the METH-induced decrease in DA uptake and inhibit the METH-induced dependence (Nakajima *et al.* 2004; Niwa *et al.* 2007c, e). Moreover, given the findings on [^{3}H] DA uptake obtained using shati-AS (Niwa *et al.* 2007a) and shati-over-expressing cells (Fig. 5b), we hypothesized that shati increased DA uptake by regulating TNF-α. To address this issue, we examined expression levels of TNF-α mRNA after transfection of the vector containing shati cDNA or treatment with shati-AS.

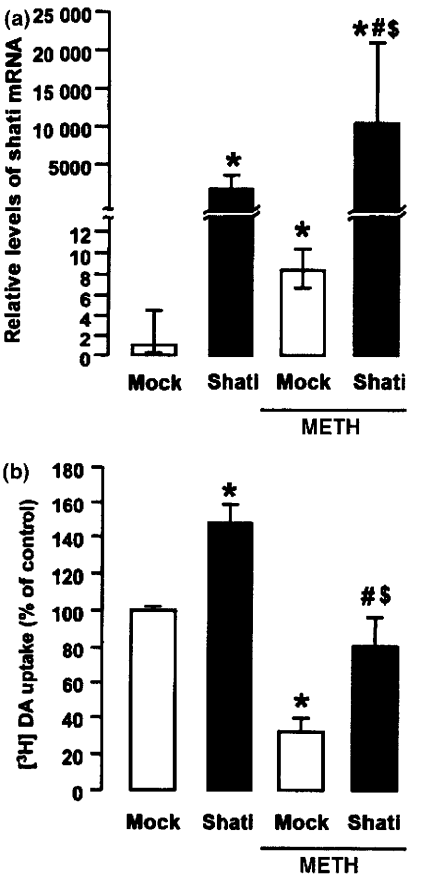

Fig. 5 Effect of overexpression of shati on DA uptake in PC12 cells. (a) Shati mRNA expression in PC12 cells transfected with the vector containing shati cDNA. The mock construct (pcDNA-DEST53), or the vector containing shati cDNA was introduced into PC12 cells. These cells were treated with 1 μM METH for 30 min. Values are means ± SE ($n = 8$). $^*p < 0.05$ versus mock-transfected cells. $^\#p < 0.05$ versus the vector containing shati cDNA-transfected cells. $^\$p < 0.05$ versus METH + mock-transfected cells. (b) Effect of over-expression of shati on [^{3}H] DA uptake in PC12 cells. The mock construct (pcDNA-DEST53), or the vector containing shati cDNA was introduced into PC12 cells. The cells were pre-treated with 1 μM METH for 30 min, and [^{3}H] DA uptake was measured. The [^{3}H] DA uptake was 0.12 ± 0.02 pmol/10 min for the mock-transfected cells. The final concentration of [^{3}H] DA was 20 nM. Values are means ± SE ($n = 10$–12). $^*p < 0.05$ versus mock-transfected cells. $^\#p < 0.05$ versus the vector containing shati cDNA-transfected cells. $^\$p < 0.05$ versus METH + mock-transfected cells.

Shati-over-expressing cells themselves had increased TNF-α mRNA expression compared with the mock-transfected cells (Fig. 6a left two columns), suggesting that shati regulates expression of TNF-α in PC12 cells. The increase in TNF-α mRNA expression evoked by METH treatment (1 μM, 30 min) in mock-transfected cells was significantly potentiated by overexpression of shati *in vitro* (drug, $F_{1,28} = 21.000$, $p < 0.01$; transfection, $F_{1,28} = 65.860$,

$p < 0.01$; drug × transfection, $F_{1,28} = 3.557$, $p = 0.070$; two-way ANOVA) (Fig. 6a right two columns). As shown in Fig. 6b right three columns, the increase in TNF-α mRNA expression evoked by repeated METH treatment in the NAc was significantly abolished by shati-AS, although shati-SC had no effect. Moreover, TNF-α mRNA expression in the NAc of saline-treated mice was also inhibited by shati-AS, although not by shati-SC (drug, $F_{1,47} = 48.473$, $p < 0.01$; intracerebroventricular treatment, $F_{2,47} = 15.670$, $p < 0.01$; drug × intracerebroventricular treatment, $F_{2,47} = 0.239$, $p = 0.788$; two-way ANOVA) (Fig. 6b left three columns), indicating that shati-AS decreases effectively the expression of TNF-α mRNA through the down-regulation of shati mRNA expression.

As shown in Fig. 6c, right four columns, the ameliorative effect of shati on the METH-induced decrease in DA uptake

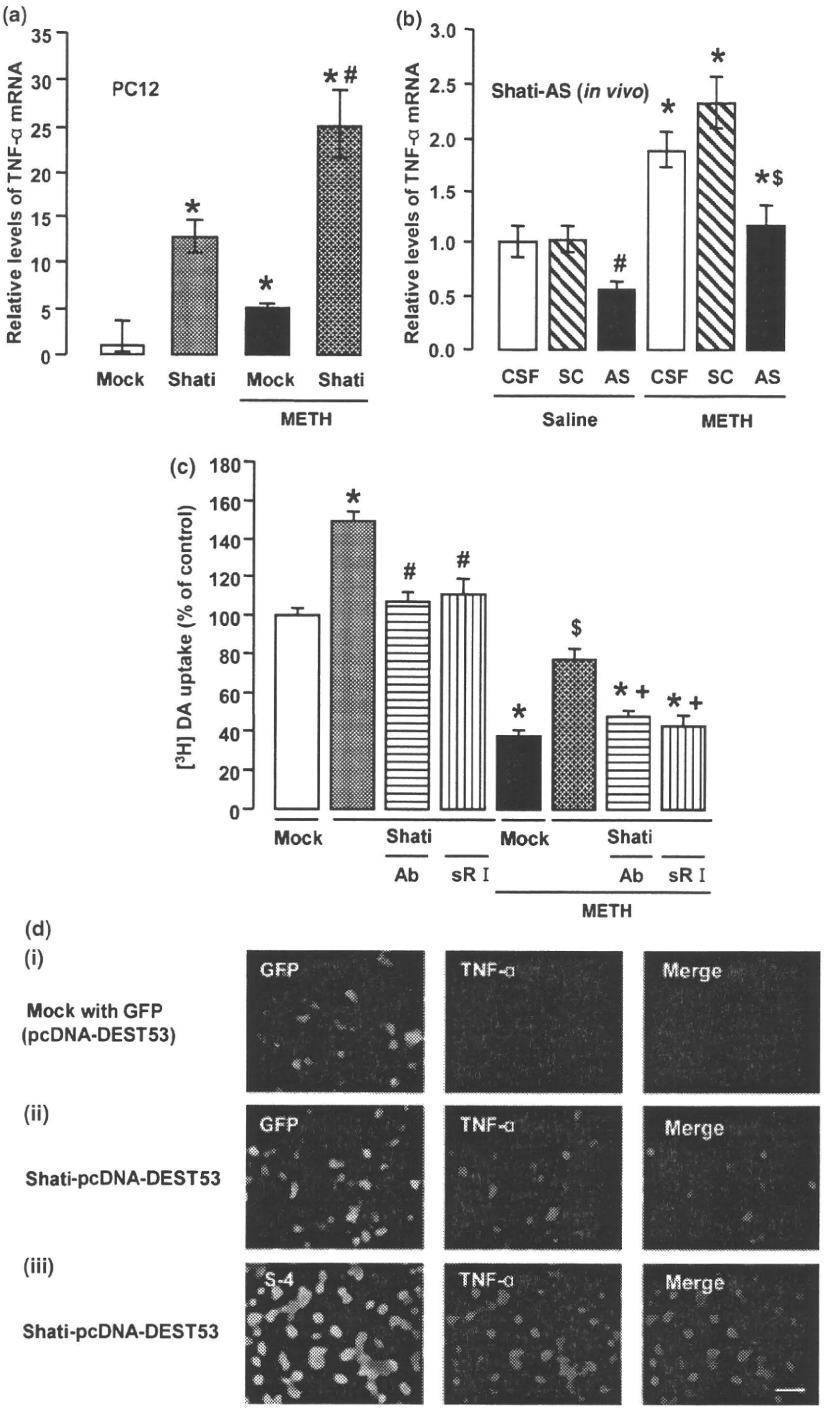

was antagonized by treatment with the TNF-αantibody (50 ng/mL) or soluble TNF receptor I (1 ng/mL). The shati-induced potentiation of DA uptake was also inhibited by the treatments in shati-over-expressing cells (drug, $F_{1,72} = 296.090$, $p < 0.01$; transfection, $F_{1,72} = 13.864$, $p < 0.01$; neutralization, $F_{1,72} = 32.930$, $p < 0.01$; drug × transfection, $F_{1,72} = 0.189$, $p = 0.665$; drug × neutralization, $F_{1,72} = 1.496$, $p = 0.225$; transfection × neutralization, $F_{1,72} = 34.828$, $p < 0.01$; drug × transfection × neutralization, $F_{1,72} = 0.003$, $p = 0.958$; three-way ANOVA) (Fig. 6c left four columns). These results suggest that over-expression of shati increased DA uptake by regulating TNF-α in PC12 cells. To confirm the relationship between shati and TNF-α, we examined immunostaining for GFP, which is co-expressed with shati, or S-4 and TNF-α. The cells mock-transfected, which express GFP, but not shati, were immunopositive for GFP, but not TNF-α. The cells transfected with the vector containing shati cDNA, which express both GFP and shati, were immunopositive for GFP or S-4 and TNF-α. The cells immunopositive for S-4 were merged with those positive for TNF-α. These results indicated that shati was expressed in TNF-α-immunopositive cells (Fig. 6d).

Discussion

DA is the predominant catecholamine neurotransmitter in the CNS. Disruptions of DA signaling contribute to various psychiatric and neurological disorders, including drug addiction, schizophrenia, and Parkinson's disease (Self and Nestler 1995; Hyman 1996). Extracellular DA levels are primarily regulated by DAT, an integral membrane protein that is a member of the Na^+/Cl^--dependent co-transporter gene family (Amara and Kuhar 1993). By removing extracellular DA and recycling it back to the neuron, DAT plays an essential role in terminating DA signaling. Pharmacological blockage of DAT by psychostimulants inhibits the reuptake of DA from the extracellular space, resulting in increased extracellular DA levels and augmented receptor stimulation (Horn 1990). Although pharmacological and genetic ablation (Grace 1995; Jones *et al.* 1998) studies indicate a critical role for DAT in the maintenance of DA neuronal homeostasis, the endogenous mechanisms regulating DAT expression and activity are poorly understood.

The PC12 cell line is derived from the rat pheochromocytoma. It is often used as an *in vitro* model to understand the physiology of central DA neurons (Roda *et al.* 1980; Tischler 2002; Fornai *et al.* 2007). A number of factors contribute to the wide use of PC12 cells: they are inexpensive as well as easy to handle, and mimic many features of central DA neurons. In fact, PC12 cells produce catecholamines (Markey *et al.* 1980; Roda *et al.* 1980; Vaccaro *et al.* 1980). In particular, they contain DA (Greene and Rein 1978) as the main catecholamine and bear DA receptors on their external membrane (Sampath *et al.* 1994). In light of the presence of DA and DA receptors, as well as DA uptake mechanisms, PC12 cell lines are considered to be closer to DA terminals than their ancestors (i.e. chromaffin cells of the adrenal medulla). This concept is reinforced by the presence of monoamine oxidase type A, which also characterizes DA neurons (Finberg and Youdim 1983), in contrast with the established prevalence of monoamine oxidase type B within chromaffin cells of the adrenal medulla (Youdim 1991).

Recently, we have demonstrated that TNF-α and its inducer play a neuroprotective role in the behavioral sensitization to and rewarding effects of METH by activating plasmalemmal and vesicular DAT as well as by inhibiting the METH-induced increase in extracellular DA levels (Nakajima *et al.* 2004; Niwa *et al.* 2007c,e). TNF-α modulates cellular responses through the ERK1/2 and NF-κB signaling pathways (van Vliet *et al.* 2005). The adaptor protein TNF receptor-associated factor 2 (TRAF2) and the serine and threonine protein kinase receptor-interacting protein are required for optimal TNF-induced signaling through ERK1/2, c-Jun N-termial kinase (JNK) and p38 mitogen-activated

Fig. 6 Involvement of TNF-α in shati-induced increase in DA uptake in PC12 cells. (a) TNF-α mRNA expression in PC12 cells transfected with the vector containing shati cDNA. The expression vector alone (pcDNA-DEST53), or the vector containing shati cDNA was introduced into PC12 cells. The cells were treated with 1 μM METH for 30 min. Values are means ± SE ($n = 8$). $^*p < 0.05$ versus mock-transfected group. $^\#p < 0.05$ versus METH + mock-transfected group. (b) Effect of shati-AS on TNF-α mRNA expression. Mice were administered METH (1 mg/kg, s.c.) for 5 days and decapitated 2 h after the final treatment. Values are means ± SE ($n = 8$–10). $^*p < 0.05$ versus corresponding saline-treated mice. $^\#p < 0.05$ versus saline + CSF and saline + shati-SC-treated mice. $^\$p < 0.05$ versus METH + CSF and METH + shati-SC-treated mice. (c) Involvement of TNF-α in shati-induced increase in [^{3}H] DA uptake in PC12 cells. The expression vector alone (pcDNA-DEST53), or the vector containing shati cDNA was introduced into PC12 cells. The cells were pre-treated with anti-TNF-α antibody (Ab; 50 ng/mL) or soluble TNF receptor I (sR I; 1 ng/mL) 10 min before their treatment with METH (1 μM, 30 min), and assayed for [^{3}H] DA uptake. The [^{3}H] DA uptake was 0.15 ± 0.02 pmol/10 min for the mock-transfected group. The final concentration of [^{3}H] DA was 20 nM. Values are means ± SE ($n = 10$). $^*p < 0.05$ versus mock-transfected group. $^\#p < 0.05$ versus the vector containing shati cDNA-transfected group. $^\$p < 0.05$ versus METH + mock-transfected group. $^+p < 0.05$ versus METH + the vector containing shati cDNA-transfected group. (d) Immunostaining of shati and TNF-α in PC12 cells transfected with the vector containing shati cDNA. The expression vector alone (pcDNA-DEST53) (i), or the vector containing shati cDNA (ii) (iii) was introduced into PC12 cells. The GFP or shati-immunopositive cells (green) were co-localized with TNF-α-immunopositive cells (red) (ii) (iii). Double immunostaining for GFP or S-4 and TNF-α in PC12 cells transfected with the vector containing shati cDNA reveals expression of shati in TNF-α-immunopositive cells (ii) (iii). Scale bar: 20 μm.

protein kinase (p38) (Baud and Karin 2001; Devin *et al.* 2003). MEK inhibitor PD98059 significantly decreases phosphorylated ERK1/2 without affecting total ERK level, MEK-JNK, -p38, and -NF-κB, resulting in loss of DAT surface expression and DAT capacity. According these results, MEK-ERK pathway, but not MEK-JNK, -p38, or -NF-κB pathway, is important for intracellular trafficking and transport capacity of DAT (Morón *et al.* 2003). Therefore, we investigated the involvement of TNF-α in DA uptake and the METH-induced inhibition of DA uptake in PC12 cells. Moreover, we examined the involvement of MEK-ERK signaling in the effects of TNF on DA uptake. TNF-α increased DA uptake via the MEK-ERK signaling pathway in PC12 cells (Figs 1 and 2). The increase was antagonized by the anti-TNF-α antibody and soluble TNF receptor I (Fig. 1b and c), suggesting that TNF-α certainly increases DA uptake in PC12 cells. Moreover, TNF-α inhibited the METH-induced decrease in DA uptake in PC12 cells (Fig. 3b). We have previously reported that the kinetics of [^{3}H] DA uptake in the absence or presence of TNF-α (10 ng/mL). Lineweaver-burk plots show that TNF-α potentiates [^{3}H] DA uptake by increasing the affinity (Km) accompanied by reducing the maximum number of [^{3}H] DATs (Vmax) (Nakajima *et al.* 2004). We suggest that TNF-α modulates the function of DAT, although it also regulates the expression of DAT. The expression of TNF-α is induced through the activation of transcription factors such as activator protein-1 (AP-1) and NF-κB by the activation of JNK/p38 (Guha *et al.* 2000; Rahman and MacNee 2000). Further, TNF-α acts on mitochondria to generate reactive oxygen species, which are involved in the activation of AP-1 and NF-κB (Rahman and MacNee 2000). Changes in transcription factors may result in long-term changes in gene expression, thereby contributing to neuronal adaptations that underlie behavioral sensitization (Nestler 2001). Therefore, we hypothesized that TNF-α inhibits the METH-induced increase in extracellular DA levels in the NAc by promoting DA uptake and finally inhibits METH-induced sensitization and rewarding effects (Nakajima *et al.* 2004; Niwa *et al.* 2007c,e).

'Shati', named after the symbol for Nagoya castle, was identified among molecules whose expression was regulated in the NAc of mice treated with METH (Niwa *et al.* 2007a). Recently, we have demonstrated that blockage of shati expression by shati-AS potentiates the increase in extracellular DA levels in the NAc and the decrease in synaptosomal and vesicular DA uptake in the midbrain induced by repeated METH treatment (Niwa *et al.* 2007a). Both TNF-α and shati increase DA uptake and inhibit the METH-induced decrease in DA uptake (Nakajima *et al.* 2004; Niwa *et al.* 2007a). Therefore, we investigated the precise mechanism of the effects of shati on DA uptake, and the METH-induced inhibition of DA uptake in PC12 cells. Moreover, we examined the relationship between shati and TNF-α in PC12 cells. Over-expression of shati by transfection of the vector containing shati cDNA (Fig. 4) dramatically induced the expression of shati mRNA (Fig. 5a) and TNF-α mRNA (Fig. 6a) in PC12 cells. No histological or mechanical disruption was produced by transfection of the vector (Fig. 4a). Over-expression of shati (Fig. 5a), which occurs in TNF-α-immunopositive cells (Fig. 6d), potentiated DA uptake and inhibited the METH-induced decrease in DA uptake (Fig. 5b) in PC12 cells by regulating TNF-α expression (Fig. 6a), since these effects were antagonized by anti-TNF-α antibody and soluble TNF receptor I used for the neutralization of TNF-α (Fig. 6c; Barone *et al.* 1997). These findings strongly suggest that the over-expression of shati elicited by METH serves as a homeostatic mechanism that prevents behavioral sensitization and rewarding effects by attenuating the METH-induced increase in extracellular DA

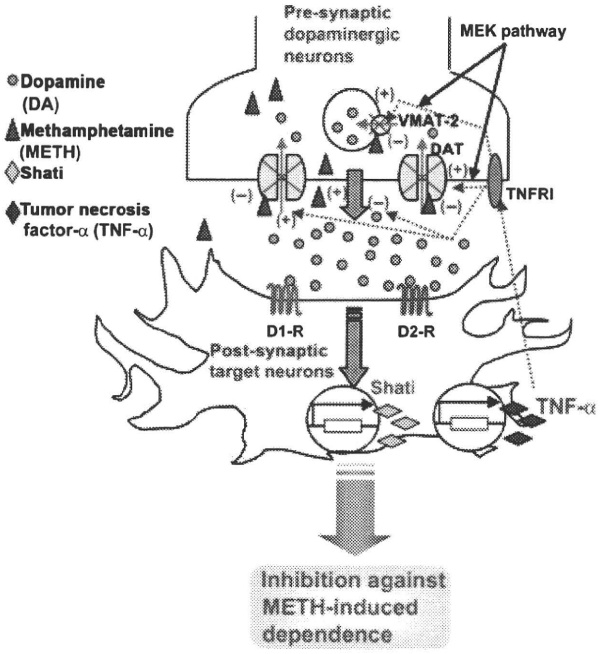

Fig. 7 Schema for regulation of TNF-α induced by shati on METH-induced DA responses. Under basal conditions, plasmalemmal DAT is involved in the reuptake of extracellular DA into the cytosol; subsequently the cytosolic DA is stored into synaptic vesicles via VMAT-2. Treatment of METH inhibits DA uptake through DA transporter and facilitates DA's release from pre-synaptic nerve terminals. METH is associated with an increase in extracellular DA levels in the brain, resulting in potentiation of the METH-induced dependence. METH induces shati and TNF-α expression in target neurons through the activation of DA receptors. TNF-α regulated by shati inhibits the METH-induced increase in extracellular DA levels in the nucleus accumbens by promoting DA uptake via MEK pathway and finally inhibits sensitization to and the rewarding effects of METH. DA: dopamine, METH: methamphetamine, TNF-α: tumor necrosis factor-α, D1-R: dopamine D1 receptor, D2-R: dopamine D2 receptor, DAT: dopamine transporter, VMAT-2: vesicular monoamine transporter-2, TNFR I: tumor necrosis factor type I receptor.

levels in the NAc through potentiation of plasmalemmal and vesicular DA uptake *via* induction of TNF-α expression (Fig. 7), although the mechanism by which TNF-α is regulated by shati remains to be elucidated.

Motif analyses have revealed that shati contains sequences of GNAT (Niwa *et al.* 2007a). Docking simulations with acetyl-CoA or ATP conducted using Molecular Operating Environment software reveal possible acetyl-CoA- and/or ATP-binding sites, since there is low potential energy for these interactions, in contrast with the prohibitively high energy of docking with DA, DNA or nuclear localization signals (Niwa *et al.* 2007a). These results suggest shati to have a physiological role in producing acetylcholine or the metabolic action of ATP. Accordingly, we have to investigate the mechanism by which shati regulates the production of acetylcholine or metabolic roles of ATP in subsequent studies.

In conclusion, we hypothesized that TNF-α expression induced by shati inhibits the METH-induced increase in extracellular DA levels in the NAc by promoting DA uptake and finally inhibits sensitization to and the rewarding effects of METH (Fig. 7). Targeting the shati-TNF-α system would provide a new therapeutic approach to the treatment of METH dependence.

Acknowledgments

This study was supported in part by Research Fellowships of the Japan Society for the Promotion of Science (JSPS) for Young Scientists; by Grants-in-aid for Scientific Research (B) and for Exploratory Research from the JSPS; by the 'Academic Frontier' Project for Private Universities (2007–2011) from the Ministry of Education, Culture, Sports, Science and Technology of Japan; by the International Research Project supported by the Meijo Asian Research Center (MARC); by Health and Labour Sciences Research on Regulatory Science of Pharmaceuticals and Medical Devices from the Ministry of Health, Labour and Welfare, Japan; by Research on Risk of Chemical Substances, Health and Labour Science Research Grants supported by the Ministry of Health, Labour and Welfare; by the Japan France Joint Health Research Program; and by the Uehara Foundation.

The authors are grateful to the Riken Cell Bank for the pheochromocytoma-12 (PC12) cells, and to Mrs. Nobuyoshi Hamada and Yoshiyuki Nakamura, Radioisotope Center Medical Branch, Nagoya University Graduate School of Medicine, for technical assistance.

References

Amara S. G. and Kuhar M. J. (1993) Neurotransmitter transporters: recent progress. *Annu. Rev. Neurosci.* **16**, 73–93.

Barone F. C., Arvin B., White R. F., Miller A., Webb C. L., Willette R. N., Lysko P. G. and Feuerstein G. Z. (1997) TNF-α. A mediator of focal ischemic brain injury. *Storoke* **28**, 1233–1244.

Baud V. and Karin K. (2001) Signal transduction by tumor necrosis factor and its relatives. *Trends Cell Biol.* **11**, 372–377. Review.

Boka G., Anglade P., Wallach D., Javoy-Agid F., Agid Y. and Hirsch E. C. (1994) Immunocytochemical analysis of tumor necrosis factor and its receptors in Parkinson's disease. *Neurosci. Lett.* **172**, 151–154.

Cen X., Nitta A., Ibi D., Zhao Y., Niwa M., Taguchi K., Hamada M., Ito Y., Ito Y., Wang L. and Nabeshima T. (2008) Identification of piccolo as a regulator of behavioral plasticity and dopamine transporter internalization. *Mol. Psychiatr.* **13**, 451–463.

Chen N. H., Reith M. E. and Quick M. W. (2004) Synaptic uptake and beyond: the sodium- and chloride-dependent neurotransmitter transporter family SLC6. *Pflugers Arch.* **447**, 519–531. Review.

Devin A., Lin Y. and Liu Z. G. (2003) The role of the death-domain kinase RIP in tumour-necrosis-factor-induced activation of mitogen-activated protein kinases. *EMBO* **4**, 623–627.

Finberg J. P. and Youdim M. B. (1983) Selective MAO A and B inhibitors: their mechanism of action and pharmacology. *Neuropharmacology* **22**, 441–446. Review.

Fog J. U., Khoshbouei H., Holy M. *et al.* (2006) Calmodulin kinase II interacts with the dopamine transporter C terminus to regulate amphetamine-induced reverse transport. *Neuron* **51**, 417–429.

Fornai F., Lenzi P., Lazzeri G., Ferrucci M., Fulceri F., Giorgi F. S., Falleni A., Ruggieri S. and Paparelli A. (2007) Fine ultrastructure and biochemistry of PC12 cells: a comparative approach to understand neurotoxicity. *Brain Res.* **1129**, 174–190.

Franklin K. B. J. and Paxinos G. (1997) *The Mouse Brain: In Stereotaxic Coordinates*. Academic Press, San Diego.

Grace A. A. (1995) The tonic/phasic model of dopamine system regulation: its relevance for understanding how stimulant abuse can alter basal ganglia function. *Drug Alcohol Depend.* **37**, 111–129. Review.

Greene L. A. and Rein G. (1978) Short-term regulation of catecholamine biosynthesis in a nerve growth factor responsive clonal line of rat pheochromocytoma cells. *J. Neurochem.* **30**, 549–555.

Guha M., Bai W., Nadler J. L. and Natarajan R. (2000) Molecular mechanisms of tumor necrosis factor α gene expression in monocytic cells via hyperglycemia-induced oxidant stress-dependent and -independent pathways. *J. Biol. Chem.* **275**, 17728–17739.

Horn A. S. (1990) Dopamine uptake: a review of progress in the last decade. *Prog. Neurobiol.* **34**, 387–400. review.

Hsu H., Xiong J. and Goeddel D. V. (1995) The TNF receptor 1-associated protein TRADD signals cell death and NF-kappa B activation. *Cell* **81**, 495–504.

Hyman S. E. (1996) Addiction to cocaine and amphetamine. *Neuron* **16**, 901–904.

Jones S. R., Gainetdinov R. R., Jaber M., Giros B., Wightman R. M. and Caron M. G. (1998) Profound neuronal plasticity in response to inactivation of the dopamine transporter. *Proc. Natl Acad. Sci. USA* **95**, 4029–4034.

Koob G. F. (1992) Drugs of abuse: anatomy, pharmacology and function of reward pathways. *Trends Pharmacol. Sci.* **13**, 177–184.

Koob G. F., Sanna P. P. and Bloom F. E. (1998) Neuroscience of addiction. *Neuron* **21**, 467–476.

Loder M. K. and Melikian H. E. (2003) The dopamine transporter constitutively internalizes and recycles in a protein kinase C-regulated manner in stably transfected PC12 cell lines. *J. Biol. Chem.* **278**, 22168–22174.

Maier S. F. and Watkins L. R. (1998) Cytokines for psychologists: implications of bidirectional immune-to-brain communication for understanding behavior, mood, and cognition. *Psychol. Rev.* **105**, 83–107.

Markey K. A., Kondo H., Shenkman L. and Goldstein M. (1980) Purification and characterization of tyrosine hydroxylase from a clonal pheochromocytoma cell line. *Mol. Pharmacol.* **17**, 79–85.

Melikian H. E. and Buckley K. M. (1999) Membrane trafficking regulates the activity of the human dopamine transporter. *J. Neurosci.* **19**, 7699–7710.

Morón J. A., Zakharova I., Ferrer J. V. *et al.* (2003) Mitogen-activated protein kinase regulates dopamine transporter surface expression and dopamine transport capacity. *J. Neurosci.* **23**, 8480–8488.

Nakajima A., Yamada K., Nagai T. *et al.* (2004) Role of tumor necrosis factor-α in methamphetamine-induced drug dependence and neurotoxicity. *J. Neurosci.* **24**, 2212–2225.

Nestler E. J. (2001) Molecular basis of long-term plasticity underlying addiction. *Nat. Rev. Neurosci.* **2**, 119–128.

Niwa M., Nitta A., Mizoguchi H., Ito Y., Noda Y., Nagai T. and Nabeshima T. (2007a) A novel molecule 'shati' is involved in methamphetamine-induced hyperlocomotion, sensitization, and conditioned place preference. *J. Neurosci.* **27**, 7604–7615.

Niwa M., Nitta A., Shen L., Noda Y. and Nabeshima T. (2007b) Involvement of glial cell line-derived neurotrophic factor in inhibitory effects of a hydrophobic dipeptide Leu-Ile on morphine-induced sensitization and rewarding effects. *Behav. Brain Res.* **179**, 167–171.

Niwa M., Nitta A., Yamada K. and Nabeshima T. (2007c) The roles of glial cell line-derived neurotrophic factor, tumor necrosis factor-α, and an inducer of these factors in drug dependence. *J. Pharmacol. Sci.* **104**, 116–121.

Niwa M., Nitta A., Yamada Y., Nakajima A., Saito K., Seishima M., Noda Y. and Nabeshima T. (2007d) Tumor necrosis factor-α and its inducer inhibit morphine-induced rewarding effects and sensitization. *Biol. Psychiatry* **62**, 658–668.

Niwa M., Nitta A., Yamada Y., Nakajima A., Saito K., Seishima M., Shen L., Noda Y., Furukawa S. and Nabeshima T. (2007e) An inducer for glial cell line-derived neurotrophic factor and tumor necrosis factor-α protects against methamphetamine-induced rewarding effects and sensitization. *Biol. Psychiatry* **61**, 890–901.

Niwa M., Yan Y. and Nabeshima T. (2008) Genes and molecules that can potentiate or attenuate psychostimulant dependence: relevance of data from animal models to human addiction. *Ann. NY Acad. Sci.* **1141**, 76–95.

Rahman I. and MacNee W. (2000) Regulation of redox glutathione levels and gene transcription in lung inflammation: therapeutic approaches. *Free Radic. Biol. Med.* **28**, 1405–1420.

Rawson R. A., Gonzales R. and Brethen P. (2002) Treatment of methamphetamine use disorders: an update. *J. Subst. Abuse Treat.* **23**, 145–150. Review.

Roda L. G., Nolan J. A., Kim S. U. and Hogue-Angeletti R. A. (1980) Isolation and characterization of chromaffin granules from a pheochromocytoma (PC 12) cell line. *Exp. Cell Res.* **128**, 103–109.

Sampath D., Jackson G. R., Werrbach-Perez K. and Perez-Polo J. R. (1994) Effects of nerve growth factor on glutathione peroxidase and catalase in PC12 cells. *J. Neurochem.* **62**, 2476–2479.

Self D. W. and Nestler E. J. (1995) Molecular mechanisms of drug reinforcement and addiction. *Annu. Rev. Neurosci.* **18**, 463–495. Review.

Sulzer D., Sonders M. S., Poulsen N. W. and Galli A. (2005) Mechanisms of neurotransmitter release by amphetamines: a review. *Prog. Neurobiol.* **75**, 406–433.

Tischler A. S. (2002) Chromaffin cells as models of endocrine cells and neurons. *Ann. NY Acad. Sci.* **971**, 366–370. Review.

Torres G. E., Gainetdinov R. R. and Caron M. G. (2003) Plasma membrane monoamine transporters: structure, regulation and function. *Nat. Rev. Neurosci.* **4**, 13–25. Review.

Vaccaro K. K., Liang B. T., Perelle B. A. and Perlman R. L. (1980) Tyrosine 3-monooxygenase regulates catecholamine synthesis in pheochromocytoma cells. *J. Biol. Chem.* **255**, 6539–6541.

Vassalli P. (1992) The pathophysiology of tumor necrosis factors. *Annu. Rev. Immunol.* **10**, 411–452. Review.

van Vliet C., Bukczynska P. E., Puryer M. A., Sadek C. M., Shields B. J., Tremblay M. L. and Tiganis T. (2005) Selective regulation of tumor necrosis factor-induced Erk signaling by Src family kinases and the T cell protein tyrosine phosphatase. *Nat. Immunol.* **6**, 253–260.

Wada R., Tifft C. J. and Proia R. L. (2000) Microglial activation precedes acute neurodegeneration in Sandhoff disease and is suppressed by bone marrow transplantation. *Proc. Natl Acad. Sci. USA* **97**, 10954–10959.

Wise R. A. (1996) Neurobiology of addiction. *Curr. Opin. Neurobiol.* **6**, 243–251.

Youdim M. B. (1991) PC12 cells as a window for the differentiation of neural crest into adrenergic nerve ending and adrenal medulla. *J. Neural Transm. Suppl.* **34**, 61–67.

Behavioural Brain Research 202 (2009) 114–121

Contents lists available at ScienceDirect

Behavioural Brain Research

journal homepage: www.elsevier.com/locate/bbr

Research report

Behavioral abnormality and pharmacologic response in social isolation-reared mice

Hiroyuki Koike[a,b], Daisuke Ibi[a], Hiroyuki Mizoguchi[c], Taku Nagai[a], Atsumi Nitta[a], Kazuhiro Takuma[d], Toshitaka Nabeshima[e], Yukio Yoneda[b], Kiyofumi Yamada[a,f,*]

[a] Department of Neuropsychopharmacology and Hospital Pharmacy, Nagoya University Graduate School of Medicine, Nagoya 466-8560, Japan
[b] Laboratory of Molecular Pharmacology, Graduate School of Natural Science and Technology, Kanazawa University, Kanazawa 920-1192, Japan
[c] Futuristic Environmental Simulation Center, Research Institute of Environmental Medicine, Nagoya University, Nagoya 464-8601, Japan
[d] Laboratory of Medicinal Pharmacology, Graduate School of Pharmaceutical Sciences, Osaka University, Suita, Osaka 565-0871, Japan
[e] Department of Chemical Pharmacology, Graduate School of Pharmaceutical Sciences, Meijo University, Nagoya 468-8503, Japan
[f] CREST, JST, Nagoya 466-8560, Japan

ARTICLE INFO

Article history:
Received 16 February 2009
Received in revised form 11 March 2009
Accepted 17 March 2009
Available online 31 March 2009

Keywords:
Social isolation
Methylphenidate
Clozapine
Fluoxetine
Aggressive behavior
Anxiety-like behavior
Social interaction

ABSTRACT

Social isolation (SI) rearing in rodents causes a variety of behavioral changes, including hyperlocomotion, anxiety, impulsivity, aggression, and learning and memory deficits. These behavioral abnormalities in rodents may be related to the symptoms in patients with neuropsychiatric disorders, such as attention-deficit hyperactivity disorder, obsessive-compulsive disorder, autism, schizophrenia and depression. In this study, we examined the effect of long-term SI rearing after weaning on emotional behaviors and cognitive function in mice. Furthermore, the effects of methylphenidate (MPH), clozapine (CLZ) and fluoxetine (FLX) on SI-induced behavioral changes were examined to measure the predictive validity of SI-reared mice as an animal model for these neuropsychiatric disorders. MPH improved SI-induced anxiety-like behavior in the elevated-plus maze test, but had no effect on aggressive behavior. In contrast, CLZ ameliorated aggressive behavior, but not anxiety-like behavior in SI-reared mice. Repeated FLX treatment prevented SI-induced aggressive behavior and social interaction deficits. These findings suggest that SI-induced behavioral abnormality is a psychobehavioral complex relevant to various clinical symptoms observed in neuropsychiatric disorders and that SI-reared mice are a useful animal model to study the pathophysiology/pathogenesis of these diseases.

1. Introduction

Adverse early life experiences, such as maternal separation or social isolation (SI) affect structural and functional brain development and adult behaviors in rodents [22,31,38]. Behavioral changes induced by SI rearing have been characterized, including enhanced locomotor activity under a novel environment [47,49], anxiety-like behavior [23,48], aggressive behavior [24,29,50], and impairment of prepulse inhibition of the acoustic startle response [9] and spatial learning and memory in the Morris water maze [24,28].

The social environment in early life significantly influences not only the behavioral organization but also neurochemical and anatomical development of the brain. For instance, dopamine and serotonin systems are affected by SI in the nucleus accumbens [20], prefrontal cortex [21] and hippocampus [33]. The neuroanatomical consequences of isolation rearing include decreased spine density of pyramidal neurons in the prefrontal cortex and hippocampus [41], fewer hippocampal synapses [46] and the decreased survival of newly divided cells and neurogenesis in the dentate gyrus of hippocampus [24].

The behavioral, neurochemical and anatomical changes in SI-reared mice may be related to clinical symptoms and pathophysiology in patients with neuropsychiatric disorders [15] in which anxiety, impulsivity and aggression are commonly observed. To address this issue, we measured the predictive validity in SI-reared mice by examining the effects of methylphenidate (MPH), clozapine (CLZ) and fluoxetine (FLX) on SI-induced behavioral abnormality. A clinical report has shown that attention-deficit/hyperactivity disorder (ADHD) occurred with disruptive disorders (oppositional defiant disorder or conduct disorder), internalizing disorder (anxiety and/or depression), or both [25]. MPH is one of the most commonly used drugs to treat ADHD [4] and is effective to improve attention and behavior, including impulsivity and aggression [34,43]. CLZ, atypical antipsychotic, is effective to reduce

* Corresponding author at: Department of Neuropsychopharmacology and Hospital Pharmacy, Nagoya University Graduate School of Medicine, 65 Tsurumai-cho, Showa-ku, Nagoya 466-8560, Japan. Tel.: +81 52 744 2674; fax: +81 52 744 2682.
E-mail address: kyamada@med.nagoya-u.ac.jp (K. Yamada).

0166-4328/$ – see front matter © 2009 Elsevier B.V. All rights reserved.
doi:10.1016/j.bbr.2009.03.028

aggressive or violent acts in schizophrenia and neuroleptic-resistant schizophrenia patients [17,42]. FLX, a selective serotonin reuptake inhibitor (SSRI), is used to treat depression. In addition, FLX reduces impulsive aggressive behavior in personality-disordered subjects [7]. Our findings suggest that SI-induced behavioral abnormality is a psychobehavioral complex relevant to various clinical symptoms observed in neuropsychiatric disorders, including ADHD, schizophrenia and depression, and that SI-reared mice are a useful animal model to study the pathophysiology/pathogenesis of these diseases.

2. Materials and methods

2.1. Animals

Male ICR mice 3 and 7 weeks old (Japan SLC Inc., Hamamatsu, Japan) were purchased and used for the experiments. They were housed under a standard 12-h light/dark cycle (lights on 9:00 am) at a constant temperature of 23 ± 1 °C with free access to food and water throughout the experiments. The animals were handled in accordance with the guidelines established by the Institutional Animal Care and Use Committee of Nagoya University, the Guiding Principles for the Care and Use of Laboratory Animals approved by the Japanese Pharmacological Society and the National Institutes of Health Guide for the Care and Use of Laboratory Animals.

2.2. Isolation rearing

After 3 days of acclimatization, 3-week-old mice were randomly divided into two groups: SI rearing and group-housed (GH) rearing. Mice in the SI group were individually housed in wire-topped opaque polypropylene cages (20 cm × 12 cm × 10 cm) while mice in the GH group continued to be housed under normal conditions (five per cage) in wire-topped clear plastic cages (34 cm × 22 cm × 15 cm). After 4 weeks SI, mice were subjected to behavioral analyses, as described below. During behavioral analysis, the housing conditions were maintained.

2.3. Drug administration

MPH hydrochloride (Nihon Ciba-Geigy K.K., Tokyo, Japan) and FLX (Sigma–Aldrich Co., St. Louis, MO, USA) were dissolved in saline. CLZ (Sigma–Aldrich Co.) was dissolved in a single drop of 1 N chloridric acid (HCl), diluted with saline, and neutralized by sodium bicarbonate [16]. MPH (1 and 3 mg/kg) and CLZ (0.5 and 2.5 mg/kg) were administered intraperitoneally (i.p.) 30 min before behavioral studies. Daily administration of FLX (10 mg/kg, i.p.) was started 2 weeks after SI, and continued until the end of the behavioral tests. During behavioral analysis, FLX was administered 30 min before the behavioral test [24].

2.4. Spontaneous locomotor activity under a novel environment

Locomotor activity was measured for 1 h using digital counters with an infrared detector (NS-AS01; Brain Science Idea Co., Ltd., Tokyo, Japan) in a polycarbonate box (35 cm × 30 cm × 17 cm high).

2.5. Elevated-plus maze test

The elevated-plus maze consisted of two open (25 cm × 8 cm × 0.5 cm) and two closed (25 cm × 8 cm × 20 cm) arms emanating from a common central platform (8 cm × 8 cm) to form a plus shape [32]. The entire apparatus was elevated to 50 cm above floor level and illuminated with a 20-W bulb. The test was started by placing a mouse on the central platform of the maze facing an open arm. An arm entry was defined as all four paws in the arm. The duration of time spent in any arms and number of arm entries was measured for 5 min. These data were used to calculate the percentage of duration in open arms [i.e., (duration in open arms/duration in open and closed arms) × 100].

2.6. Forced swim test

The forced swim test was carried out as described previously with minor modifications [27]. Mice were placed in a glass cylinder (20 cm high × 13.5 cm diameter) filled to a depth of 12 cm with water (24 ± 1 °C). A 3-min test per day was repeated for 5 days. Immobility time (floating) was measured. A mouse was judged to be

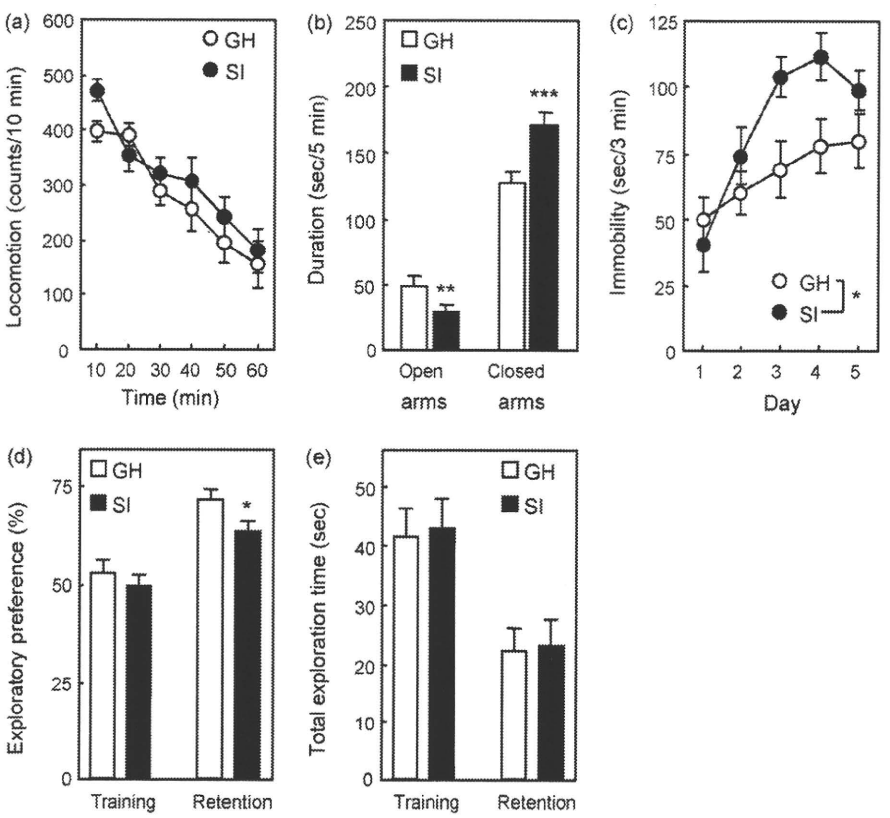

Fig. 1. Effect of social isolation (SI) rearing on emotional behavior and recognition memory. (a) Spontaneous locomotor activity under a novel environment. Locomotor activity was measured every 10 min for 60 min [group-housed (GH): $n = 10$, SI: $n = 11$]. Effect of rearing condition: $F(1,19) = 1.081$, $p = 0.3116$; effect of time (within-subject effect): $F(11,209) = 15.5$, $p < 0.001$; interaction: $F(11,209) = 1.071$, $p < 0.3861$. (b) Exploratory activity in the elevated-plus maze test. Exploratory activity was measured for 5 min (GH: $n = 17$, SI: $n = 19$). (c) Immobility in the forced swim test. Immobility was measured for 3 min per day (GH: $n = 9$, SI: $n = 10$). Effect of rearing condition: $F(1,17) = 5.228$, $p = 0.0354$; effect of day (within-subject effect): $F(4,68) = 11.821$, $p < 0.0001$; interaction: $F(4,68) = 2.316$, $p = 0.066$]. (d) Exploratory preference and (e) total exploration time in the novel object recognition test. Retention session was carried out 24 h after training (GH: $n = 14$, SI: $n = 15$). Data are shown as the means ± SE. $^*p < 0.05$, $^{**}p < 0.01$, $^{***}p < 0.001$ vs. GH mice [Student's t-test (b), (d) or ANOVA (c)].

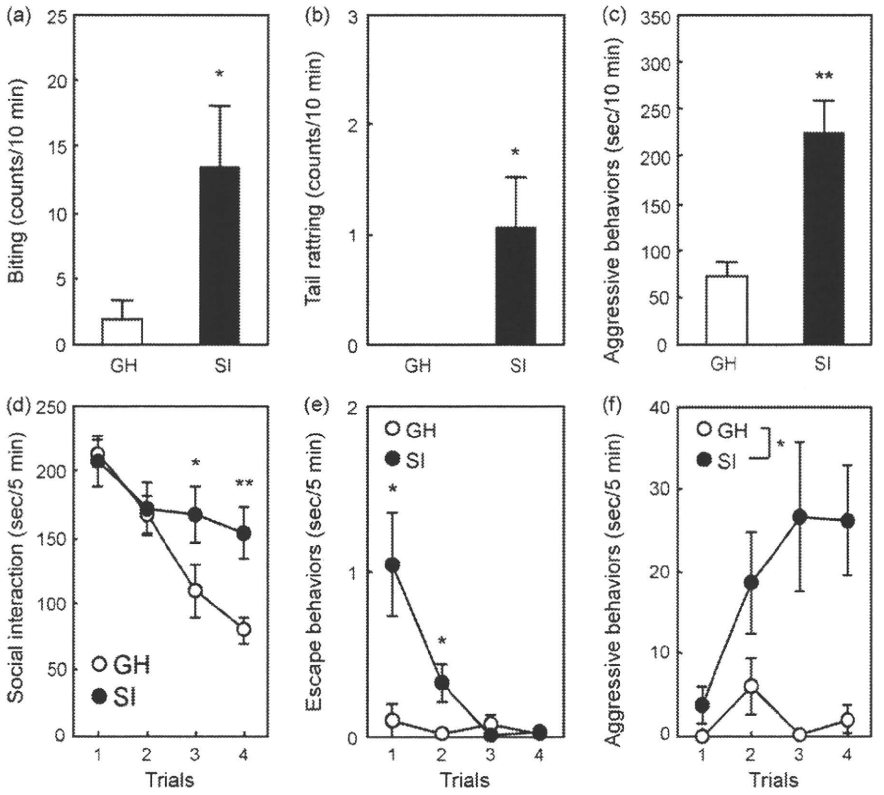

Fig. 2. Effect of social isolation (SI) rearing on aggressive and social behavior. (a–c) Aggressive behavior in the intruder-evoked aggressive test was measured for 10 min [group-housed (GH): $n = 15$, SI: $n = 15$]. (d–f) Social, escape and aggressive behavior was measured in four trials (5 min for each trial) with an intertrial interval of 30 min in the social interaction test (GH: $n = 13$, SI: $n = 15$). (d) Social interaction. Effect of rearing condition: $F(1,26) = 2.877$, $p = 0.1018$; effect of trial (within-subject effect): $F(3,78) = 25.446$, $p < 0.0001$; interaction: $F(3,111) = 6.261$, $p = 0.0007$. (e) Escape behavior. Effect of rearing condition: $F(1,26) = 8.877$, $p = 0.0062$; effect of trial (within-subject effect): $F(3,78) = 7.579$, $p = 0.0002$; interaction: $F(3.78) = 6.157$, $p = 0.0008$. (f) Aggressive behavior. Effect of rearing condition: $F(1,26) = 8.066$, $p = 0.0086$; effect of trial (within-subject effect): $F(3,78) = 4.013$, $p = 0.0104$; interaction: $F(3,78) = 1.601$, $p = 0.1959$. Data are shown as the means ± SE. $^{*}p < 0.05$, $^{**}p < 0.01$ vs. GH mice [Student's t-test (a–e) or ANOVA (f)].

immobile if it ceased struggling and remained floating motionless in water making only those movements necessary to keep its head above water.

2.7. Intruder-evoked aggressive test

The intruder-evoked aggressive test was carried out according to our previous report [24]. Male 7-week-old ICR mice were used as intruders which had not shown aggressive behavior against their peers. The resident mouse was habituated to the test cage (20 cm × 12 cm × 10 cm high) for 10 min, and then an intruder mouse was placed in the test cage. The investigating behavior of the resident mouse against the intruder was observed for 10 min. The frequency of attacking/biting and tail rattling, and duration of aggression, including attacking/biting, tail rattling, aggressive grooming, sideways posturing and pushing under were analyzed.

2.8. Social interaction test

To investigate the habituation response to a novel mouse, the social interaction test was carried out as described previously with minor modifications [44]. A male resident mouse was housed alone in a home cage (34 cm × 22 cm × 15 cm high) for 2 days before the test, and then a novel male mouse was introduced into the cage for 5 min per trial. The test consisted of four trials, in which test mice were exposed to the same novel mouse, with an intertrial interval of 30 min. We measured the time spent in social interaction (close following, inspection, anogenital sniffing, and other social body contact), escape behavior (actively avoiding the other mouse), and aggressive behavior (biting, wrestling and tail rattling).

2.9. Novel object recognition test

The novel object recognition test was carried out as described previously [35]. The experimental apparatus consisted of a Plexiglas open-field box (30 cm × 30 cm × 35 cm high), the floor of which was covered in sawdust. The apparatus was located in a sound-attenuated room and illuminated with a 20-W bulb. The test procedure consisted of three different sessions: habituation, training, and retention. Each mouse was individually habituated to the box, with 10 min exploration in the absence of objects for 3 consecutive days (habituation session, days 1–3). During the training session, two different novel objects were symmetrically fixed to the floor of the box, 8 cm from the walls, and each animal was allowed to explore in the box for 10 min (day 4). The objects were constructed from a golf ball, wooden column, and wall socket, which were different in shape and color but similar in size. The animals were considered to be exploring the object when the head of the animal was facing the object or when the animal was touching or sniffing the object. The time spent exploring each object was recorded. After training, mice were immediately returned to their home cages. During the retention sessions, the animals were placed back in the same box 24 h (day 5) after the training session, in which one of the familiar objects used during training was replaced by a novel object. The animals were then allowed to explore freely for 5 min, and the time spent exploring each object was recorded. Throughout the experiments, the objects were used in a counterbalanced manner in terms of their physical complexity and emotional neutrality. A preference index, the ratio of the amount of time spent exploring any one of the two objects (training session) or the novel object (retention session) over the total time spent exploring both objects, was used to measure cognitive function.

2.10. Statistical analysis

Statistical analyses were performed using StatView 5.0 software (SAS Institute, Cary, NC, USA). For locomotor activity, the forced swim test and social interaction test, one-way repeated measure ANOVA was used. To analyze the drug's effect, two-way or two-way repeated measures ANOVA was performed. The rearing condition, drug, and dose were between-subject factors. Time (day or trial) was a within-subject factor. Significant main effects or interactions were followed by Bonferroni's *post hoc* test. Differences between two groups were analyzed by the two-tailed Student's t-test.

3. Results

3.1. SI rearing induced behavioral abnormality

There was no significant difference in spontaneous locomotor activity between GH and SI mice under novel environmental con-

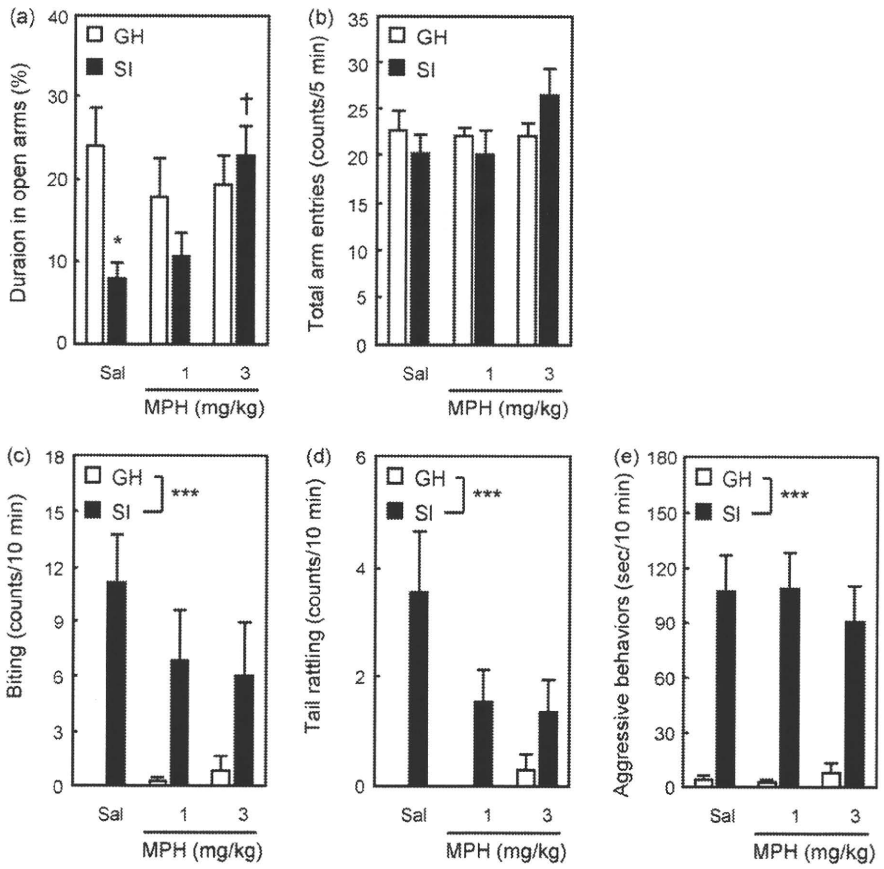

Fig. 3. Effect of methylphenidate (MPH) on social isolation (SI)-induced anxiety-like and aggressive behavior. MPH (1 or 3 mg/kg, i.p.) was administered 30 min before the behavioral test. (a–b) The elevated-plus maze test [saline-treated group-housed (GH) mice ($n = 10$); MPH (1 mg/kg)-treated GH mice ($n = 9$); MPH (3 mg/kg)-treated GH mice ($n = 10$); saline-treated SI mice ($n = 12$); MPH (1 mg/kg)-treated SI mice ($n = 10$); MPH (3 mg/kg)-treated SI mice ($n = 11$)]. (a) Duration in open arms. Effect of rearing condition: $F(1,56) = 5.238$, $p = 0.259$; effect of dose: $F(2,56) = 1.943$, $p = 0.1527$; interaction: $F(2,56) = 3.977$, $p = 0.0243$. (b) Total arm entries. Effect of rearing condition: $F(1,56) = 0.002$, $p = 0.9661$; effect of dose: $F(2,56) = 1.387$, $p = 0.2582$; interaction: $F(2,56) = 1.638$, $p = 0.2035$. (c)-(e) The intruder-evoked aggressive test [saline-treated GH mice ($n = 10$); MPH (1 mg/kg)-treated GH mice ($n = 9$); MPH (3 mg/kg)-treated GH mice ($n = 10$); saline-treated SI mice ($n = 11$); MPH (1 mg/kg)-treated SI mice ($n = 11$); MPH (3 mg/kg)-treated SI mice ($n = 11$)]. (c) Frequency of biting. Effect of rearing condition: $F(1,56) = 19.565$, $p < 0.0001$; effect of dose: $F(1,56) = 0.682$, $p = 0.5096$; interaction: $F(1,56) = 0.682$, $p = 0.5096$. (d) Frequency of tail rattling. Effect of rearing condition: $F(1,56) = 16.658$, $p = 0.0001$; effect of dose: $F(1,56) = 1.675$, $p = 0.1966$; interaction: $F(1,56) = 2.320$, $p = 0.1077$. (e) Duration of aggressive behaviors. Effect of rearing condition: $F(1,56) = 60.983$, $p < 0.0001$; effect of dose: $F(1,56) = 0.124$, $p = 0.8833$; interaction: $F(1,56) = 0.359$, $p = 0.6999$. Data are shown as the means ± SE. $^{*}p < 0.05$, $^{***}p < 0.001$ vs. GH mice [Bonferroni's *post hoc* test (a) or ANOVA (c–e)]. $^{\dagger}p < 0.05$ vs. saline-treated mice (Bonferroni's *post hoc* test).

ditions (Fig. 1a). In the elevated-plus maze test, the time spent in the open and closed arms was significantly different between GH and SI mice. SI mice spent significantly less time exploring the open arms and longer time in the closed arms than GH mice (Fig. 1b). In the forced swim test, one-way repeated ANOVA revealed a significant effect of the rearing condition on the immobility time, which was significantly increased in SI mice compared with GH mice (Fig. 1c).

In the novel object recognition test, SI rearing significantly reduced the exploratory preference to a novel object in the retention test (Fig. 1d). There was no difference in the total exploratory time in the training or retention sessions between the two groups (Fig. 1e).

In the intruder-evoked aggressive test, SI rearing significantly increased biting (Fig. 2a), tail rattling (Fig. 2b) and total time of aggressive behavior as compared with GH mice (Fig. 2c). Furthermore, GH mice showed a characteristic reduction of the time for investigating an intruder mouse. In contrast, SI mice showed little reduction in social interaction, suggesting impaired habituation to an unfamiliar intruder (Fig. 2d). SI rearing significantly increased escape behavior compared with GH mice in the first and second trials (Fig. 2e). Consistent with the result of the intruder-evoked aggressive test (Fig. 2a and b), SI mice exhibited significantly more aggressive behavior than GH mice (Fig. 2f).

3.2. MPH improved SI-induced anxiety-like behavior, but not aggressive behavior

MPH significantly ameliorated the reduced time spent in the open arms in SI mice in a dose-dependent manner (Fig. 3a) without affecting the total number of arm entries (Fig. 3b). MPH had no effect on SI-induced aggressive behavior at the dose examined (Fig. 3c), although there was a tendency for the number of biting and tail rattling in SI mice to decrease (Fig. 3a and b).

3.3. CLZ improved SI-induced aggressive behavior, but not anxiety-like behavior

CLZ (2.5 mg/kg) significantly decreased the time spent in the open arms and total arm entries in the elevated-plus maze test in both GH and SI mice (Fig. 4a and b). Furthermore, CLZ (2.5 mg/kg) completely inhibited biting and tail rattling (Fig. 4c and d) and significantly reduced the time spent in aggressive behavior (Fig. 4e) in SI mice.

3.4. Repeated FLX treatment improved SI-induced deficit of social behavior

Repeated FLX treatment significantly improved the SI-induced deficit of social behavior to the level in saline-treated GH mice with-

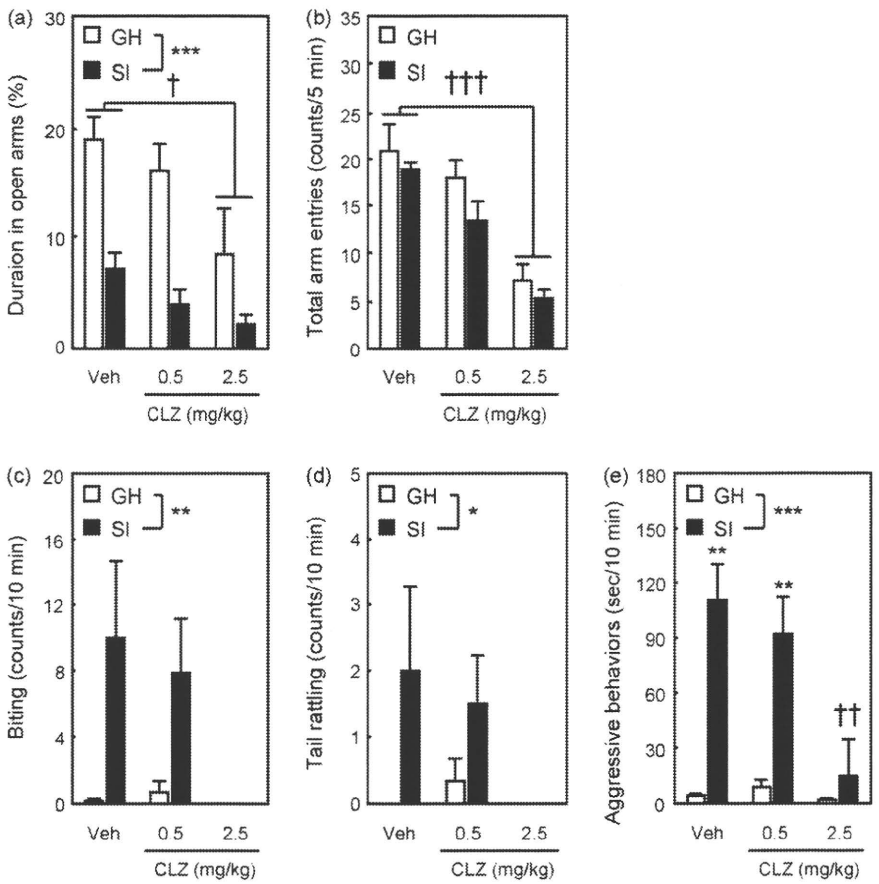

Fig. 4. Effect of clozapine (CLZ) on social isolation (SI)-induced anxiety-like and aggressive behavior. CLZ (0.5 or 2.5 mg/kg, i.p.) was administered 30 min before the behavioral test. (a–c) The elevated-plus maze test [vehicle-treated group-housed (GH) mice ($n = 6$); CLZ (0.5 mg/kg)-treated GH mice ($n = 9$); CLZ (2.5 mg/kg)-treated GH mice ($n = 9$); vehicle-treated SI mice ($n = 6$); CLZ (0.5 mg/kg)-treated SI mice ($n = 9$); CLZ (2.5 mg/kg)-treated SI mice ($n = 11$)]. (a) Duration in open arms. Effect of rearing condition: $F(1,44) = 25.47$, $p < 0.0001$; effect of dose: $F(2,44) = 5.155$, $p = 0.0097$; interaction: $F(2,44) = 1.063$, $p = 0.354$. (b) Total arm entries. Effect of rearing condition: $F(1,44) = 3.778$, $p = 0.058$; effect of dose: $F(2,44) = 30.824$, $p < 0.0001$; interaction: $F(2,44) = 0.404$, $p = 0.6702$. (c–e) The intruder-evoked aggressive test [vehicle-treated GH mice ($n = 10$); CLZ (0.5 mg/kg)-treated GH mice ($n = 9$); CLZ (2.5 mg/kg)-treated GH mice ($n = 10$); vehicle-treated SI mice ($n = 11$); CLZ (0.5 mg/kg)-treated SI mice ($n = 11$); CLZ (2.5 mg/kg)-treated SI mice ($n = 11$)]. (c) Frequency of biting. Effect of rearing condition: $F(1,43) = 10.187$, $p = 0.0026$; effect of dose: $F(1,43) = 3.282$, $p = 0.0471$; interaction: $F(1,43) = 2.757$, $p = 0.0747$. (d) Frequency of tail rattling. Effect of rearing condition: $F(1,43) = 5.382$, $p = 0.0252$; effect of dose: $F(1,43) = 2.119$, $p = 0.1325$; interaction: $F(1,43) = 1.562$, $p = 0.2215$. (e) Duration of aggressive behaviors. Effect of rearing condition: $F(1,43) = 25.9$, $p < 0.0001$; effect of dose: $F(1,43) = 5.592$, $p = 0.0069$; interaction: $F(1,43) = 4.539$, $p = 0.0163$. Data are shown as the means ± SE. $^{*}p < 0.05$, $^{**}p < 0.01$, $^{***}p < 0.001$ vs. GH mice [ANOVA (a), (c–e) or Bonferroni's *post hoc* test (e)]. $^{\dagger}p < 0.05$, $^{\dagger\dagger}p < 0.05$, $^{\dagger\dagger\dagger}p < 0.001$ vs. vehicle-treated mice [ANOVA (a)-(b) or Bonferroni's *post hoc* test (e)].

out affecting the social behavior in GH mice (Fig. 5a). Furthermore, repeated FLX treatment significantly reduced aggressive behavior in SI mice (Fig. 5c). There was a tendency for repeated FLX treatment to decrease escape behavior in SI mice, but the effect was not statistically significant (Fig. 5b).

4. Discussion

The behavioral, neurochemical and anatomical changes in SI-reared mice may be relevant to the clinical symptoms and pathophysiology in patients with neuropsychiatric disorders, such as ADHD and schizophrenia. To address this issue, we examined the response to drugs used to treat these neuropsychiatric disorders.

First, we investigated the effect of SI rearing after weaning on emotional behavior and recognition memory. SI rearing after weaning induced anxiety-like behavior, aggressive behavior, abnormal social interaction and recognition memory deficits in mice, which is consistent with previous studies reporting anxiety [23,48,51], aggression [29,50], social interaction [12,50] and recognition memory [1,47], respectively. On the other hand, some studies showed an anxiolytic-like effect of SI rearing in the elevated-plus maze test [18,47]. It is possible that SI-induced hyperactivity may be attributable to the anxiolytic-like effect under a novel environment. In our study, SI-reared mice exhibited no difference in locomotor activity and habituation response to a novel environment compared with GH mice. Under such conditions, anxiety-like behaviors were demonstrated with SI rearing.

We found that SI-reared mice were vulnerable to repeated forced swim stress. In contrast, previous reports showed that SI rearing in rodents reduced the immobility time in the forced swim test [19,27]. The discrepancy in the forced swim test may be explained by the difference in behavioral testing. In previous studies, mice were subjected to the forced swim test once or twice, while in the present study, the test was repeated on 5 consecutive days. In fact, there was no apparent difference in immobility time during the first 2 days of the test in the present study.

To assess the predictive validity of SI-reared mice as an animal model of neuropsychiatric disorders, we examined the effects of MPH, CLZ and FLX on SI-induced behavioral abnormalities. We chose the elevated-plus maze test and intruder-evoked aggressive test for MPH and CLZ experiments because anxiety-like behavior and aggressive behavior are the most distinctive alteration of behaviors induced by SI rearing, and ADHD and schizophrenic patients often exhibit anxiety and violence behavior [3,17,25]. The clinical dose range for MPH to treat ADHD is 0.3–0.6 mg/kg (twice

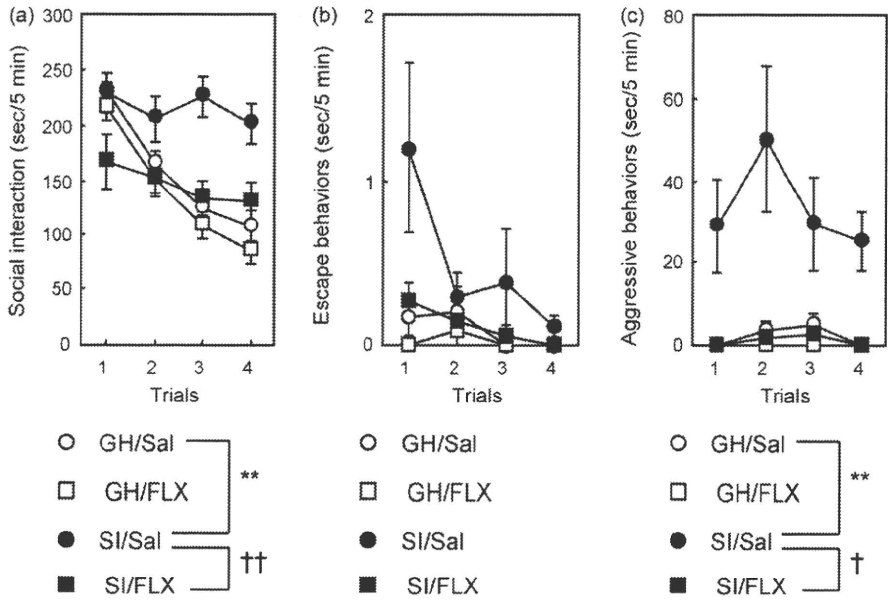

Fig. 5. Effect of repeated fluoxetine (FLX) treatment on social isolation (SI)-induced impairment of social behavior. Daily administration of FLX (10 mg/kg, i.p.) was started 2 weeks after SI and continued to the end of the social interaction test. (a) Social behavior. Effect of rearing condition: $F(1,39) = 6.448$, $p = 0.0152$; effect of drug: $F(1,39) = 11.473$, $p = 0.0016$; interaction: $F(1,39) = 4.147$, $p = 0.0485$. (b) Escape behavior. Effect of rearing condition: $F(1,39) = 2.737$, $p = 0.1061$; effect of drug: $F(1,39) = 2.211$, $p = 0.1451$; interaction: $F(1,39) = 1.050$, $p = 0.3119$. (c) Aggressive behavior. Effect of rearing condition: $F(1,39) = 4.741$, $p = 0.0356$; effect of drug: $F(1,39) = 5.191$, $p = 0.0283$; interaction: $F(1,39) = 4.160$, $p = 0.0482$. Data are shown as the means ± SE [GH/Sal: saline-treated group-housed mice ($n = 14$); GH/FLX: FLX-treated GH mice ($n = 7$); SI/Sal: saline-treated SI mice ($n = 14$); SI/FLX: fluoxetine-treated SI mice ($n = 8$)]. $^{**}p < 0.01$ vs. GH mice. $^{\dagger}p < 0.05$, $^{\dagger\dagger}p < 0.01$ vs. saline-treated mice (Bonferroni's *post hoc* test).

a day) and MPH raises resting extracellular levels of dopamine several-fold which in turn inhibits the nerve impulse-associated release [40]. Accordingly, we chose 1–3 mg/kg of MPH in this experiment. Our findings suggested that MPH could improve SI-induced anxiety-like behavior because the drug increased the reduced time spent in open arms in SI mice without affecting the time in GH mice. It is unlikely that the anxiolytic effect arises from hyperlocomotion in MPH-treated mice since total arm entries in both GH and SI mice were not affected by MPH. Previous studies demonstrated that SI rearing in rats altered the time course of locomotor activity induced by amphetamine [26] and increased amphetamine-induced dopamine release in the nucleus accumbens [20]. Therefore, functional changes in dopaminergic systems may be involved in anxiety-like behavior in SI-reared mice as well as the anxiolytic effect of MPH. In the present study, MPH had little effect on SI-induced aggressive behavior, which disagrees with the previous study that MPH inhibited aggression in SI mice [29]. The reason for the discrepancy between studies is unclear at present. Higher doses of MPH may be required to inhibit SI-induced aggressive behavior.

A previous study demonstrated that CLZ at a dose of 2.5 mg/kg reduced aggressive behavior in isolated mice [30]. Consistently, we found that CLZ at same dose markedly suppressed aggressive behavior although it had little effect on anxiety-like behavior in SI-reared mice. However, the anti-aggressive effect of CLZ may be attributed to sedation, because CLZ treatment decreased the number of total arm entries in the elevated-plus maze test. In fact, CLZ at dose of 2.5 mg/kg significantly reduced locomotor activity in both GH and SI mice (data not shown). CLZ has affinities for and antagonizes dopamine (DA) and serotonin (5-HT) receptors. The neurotransmitters DA, 5-HT and gamma-aminobutyric acid have been implicated in the neurobiological mechanisms of aggression [10]. Previous studies showed that the extracellular DA level was increased in the nucleus accumbens during and after aggressive episode in rats [13], while a D1-like antagonist (SCH-23390) or a D2-like antagonist (sulpiride) microinjected into the nucleus accumbens decreased the positive reinforcing properties of aggression in mice [8]. Furthermore, SI rearing induces hyperfunction of the mesolimbic dopaminergic system [15]. Thus, the dopaminergic hyperfunction induced by SI rearing may play a role in the development of aggressive behavior.

The 5-HT system has a role in aggressive behavior [10,36]. Previous studies showed an inverse correlation between the tendency to engage in aggression and a defect of serotonergic neurons in not only rodents [6] but also humans [45]. In accord with this evidence, FLX ameliorated impulsive aggressive behavior in personality-disordered subjects [7] and rodents [14,24]. We have previously reported that a single FLX treatment (10 mg/kg) failed to reverse SI-induced aggressive behavior in the intruder-evoked aggressive test and anxiety-like behavior in the elevated-plus maze, but the aggressive behavior was ameliorated by repeated FLX treatment (10 mg/kg) [24]. Accordingly, in this study social interaction test was conducted to assess the effect of repeated FLX treatment on SI-induced impairment of social behavior. We found that FLX ameliorated the impairment of social behavior as well as aggressive behavior in SI-reared mice. A recent study demonstrated that FLX suppressed the activation of neuronal circuits of aggression during aggressive interaction [14]. The extracellular 5-HT level is decreased in the prefrontal cortex (PFC) during and following aggressive conflict in rats [13]. The 5-HT_{1A} or 5HT_{1B} receptor agonist microinjected in the PFC decreases aggression [5,11]. On the other hand, SI rearing induces the dysfunction of serotonergic neurons; for example, 5-HT_{1A} receptor binding is significantly reduced in the PFC of SI-reared rodents [37,39]. Brain dialysis revealed that 5-HT release induced by KCl in the frontal cortex was attenuated in SI rats [2]. Hence, aggression in SI-reared mice may be attributed to the hypofunction of serotonergic neurons in the brain, especially in the PFC.

In the present study, we showed that long-term SI rearing after weaning affected adult behavior in mice. SI-reared mice exhibited increased vulnerability to swim stress, increased anxiety and impulsivity/aggression, and impaired recognition memory and social interaction. MPH improved SI-induced anxiety

behavior, CLZ reduced SI-induced aggressive behavior, and repeated FLX treatment ameliorated SI-induced abnormality of social behavior. These results suggest that SI-induced behavioral abnormality is a psychobehavioral complex relevant to various clinical symptoms observed in neuropsychiatric disorders, including ADHD, schizophrenia and depression, and that SI-reared mice are valuable to analyze the pathophysiology/pathogenesis of these diseases.

Acknowledgments

This study was supported in part by a Grant-in-Aid for Scientific Research (no.19390062) from the JSPS, the global COE program from the Ministry of Education, Culture, Sports, Science and Technology of Japan, the Academic Frontier Project for Private Universities; matching fund subsidy from MEXT, 2007–2011, the Research on Risk of Chemical Substances, Health and Labour Science Research Grants supported by Ministry of Health, Labour and Welfare, Takeda Science Foundation, AstraZeneca Research Grant 2008, and JST, CREST.

References

[1] Bianchi M, Fone KF, Azmi N, Heidbreder CA, Hagan JJ, Marsden CA. Isolation rearing induces recognition memory deficits accompanied by cytoskeletal alterations in rat hippocampus. Eur J Neurosci 2006;24:2894–902.
[2] Bickerdike MJ, Wright IK, Marsden CA. Social isolation attenuates rat forebrain 5-HT release induced by KCl stimulation and exposure to a novel environment. Behav Pharmacol 1993;4:231–6.
[3] Braga RJ, Petrides G, Figueira I. Anxiety disorders in schizophrenia. Compr Psychiatry 2004;45:460–8.
[4] Castellanos FX, Tannock R. Neuroscience of attention-deficit/hyperactivity disorder: the search for endophenotypes. Nat Rev Neurosci 2002;3:617–28.
[5] Centenaro LA, Vieira K, Zimmermann N, Miczek KA, Lucion AB, de Almeida RM. Social instigation and aggressive behavior in mice: role of 5-HT(1A) and 5-HT (1B) receptors in the prefrontal cortex. Psychopharmacology (Berl) 2008;201:237–48.
[6] Chiavegatto S, Nelson RJ. Interaction of nitric oxide and serotonin in aggressive behavior. Horm Behav 2003;44:233–41.
[7] Coccaro EF, Kavoussi RJ, Fluoxetine. impulsive aggressive behavior in personality-disordered subjects. Arch Gen Psychiatry 1997;54:1081–8.
[8] Couppis MH, Kennedy CH. The rewarding effect of aggression is reduced by nucleus accumbens dopamine receptor antagonism in mice. Psychopharmacology (Berl) 2008;197:449–56.
[9] Day-Wilson KM, Jones DN, Southam E, Cilia J, Totterdell S. Medial prefrontal cortex volume loss in rats with isolation rearing-induced deficits in prepulse inhibition of acoustic startle. Neuroscience 2006;141:1113–21.
[10] de Almeida RM, Ferrari PF, Parmigiani S, Miczek KA. Escalated aggressive behavior: dopamine, serotonin and GABA. Eur J Pharmacol 2005;526:51–64.
[11] de Almeida RM, Rosa MM, Santos DM, Saft DM, Benini Q, Miczek KA. 5-HT(1B) receptors, ventral orbitofrontal cortex, and aggressive behavior in mice. Psychopharmacology (Berl) 2006;185:441–50.
[12] Ferdman N, Murmu RP, Bock J, Braun K, Leshem M. Weaning age, social isolation, and gender, interact to determine adult explorative and social behavior, and dendritic and spine morphology in prefrontal cortex of rats. Behav Brain Res 2007;180:174–82.
[13] Ferrari PF, van Erp AM, Tornatzky W, Miczek KA. Accumbal dopamine and serotonin in anticipation of the next aggressive episode in rats. Eur J Neurosci 2003;17:371–8.
[14] Ferris CF, Stolberg T, Kulkarni P, Murugavel M, Blanchard R, Blanchard DC, et al. Imaging the neural circuitry and chemical control of aggressive motivation. BMC Neurosci 2008;9:111–6.
[15] Fone KC, Porkess MV. Behavioural and neurochemical effects of post-weaning social isolation in rodents-relevance to developmental neuropsychiatric disorders. Neurosci Biobehav Rev 2008;32:1087–102.
[16] Frau R, Orrù M, Fà M, Casti A, Manunta M, Fais N, et al. Effects of topiramate on the prepulse inhibition of the acoustic startle in rats. Neuropsychopharmacology 2007;32:320–31.
[17] Glazer WM, Dickson RA. Clozapine reduces violence and persistent aggression in schizophrenia. J Clin Psychiatry 1998;59:8–14.
[18] Guo M, Wu CF, Liu W, Yang JY, Chen D. Sex difference in psychological behavior changes induced by long-term social isolation in mice. Prog Neuropsychopharmacol Biol Psychiatry 2004;28:115–21.
[19] Hall FS, Huang S, Fong GF, Pert A. The effects of social isolation on the forced swim test in Fawn hooded and Wistar rats. J Neurosci Methods 1998;79:47–51.
[20] Hall FS, Wilkinson LS, Humby T, Inglis W, Kendall DA, Marsden CA, et al. Isolation rearing in rats: pre- and postsynaptic changes in striatal dopaminergic systems. Pharmacol Biochem Behav 1998;59:859–72.
[21] Heidbreder CA, Weiss IC, Domeney AM, Pryce C, Homberg J, Hedou G, et al. Behavioral, neurochemical and endocrinological characterization of the early social isolation syndrome. Neuroscience 2000;100:749–68.
[22] Heim C, Plotsky PM, Nemeroff CB. Importance of studying the contributions of early adverse experience to neurobiological findings in depression. Neuropsychopharmacology 2004;29:641–8.
[23] Hellemans KG, Benge LC, Olmstead MC. Adolescent enrichment partially reverses the social isolation syndrome. Brain Res Dev Brain Res 2004;150:103–15.
[24] Ibi D, Takuma K, Koike H, Mizoguchi H, Tsuritani K, Kuwahara Y, et al. Social isolation rearing-induced impairment of the hippocampal neurogenesis is associated with deficits in spatial memory and emotion-related behaviors in juvenile mice. J Neurochem 2008;105:921–32.
[25] Jensen PS, Hinshaw SP, Kraemer HC, Lenora N, Newcorn JH, Abikoff HB, et al. ADHD comorbidity findings from the MTA study: comparing comorbid subgroups. J Am Acad Child Adolesc Psychiatry 2001;40:147–58.
[26] Jones GH, Hernandez TD, Kendall DA, Marsden CA, Robbins TW. Dopaminergic and serotonergic function following isolation rearing in rats: study of behavioural responses and postmortem and in vivo neurochemistry. Pharmacol Biochem Behav 1992;43:17–35.
[27] Karolewicz B, Paul IA. Group housing of mice increases immobility and antidepressant sensitivity in the forced swim and tail suspension tests. Eur J Pharmacol 2001;415:197–201.
[28] Lu L, Bao G, Chen H, Xia P, Fan X, Zhang J, et al. Modification of hippocampal neurogenesis and neuroplasticity by social environments. Exp Neurol 2003;183:600–9.
[29] Miczek KA, O'Donnell JM. Intruder-evoked aggression in isolated and nonisolated mice: effects of psychomotor stimulants and L-dopa. Psychopharmacology (Berl) 1978;57:47–55.
[30] Millan MJ, Brocco M, Gobert A, Schreiber R, Dekeyne A. S-16924 [(R)-2-[1-[2-(2,3-dihydro-benzo[1,4]dioxin-5-yloxy)-ethyl]-pyrrolidin-3yl]-1-(4-fluorophenyl)-ethanone], a novel, potential antipsychotic with marked serotonin1A agonist properties: III. Anxiolytic actions in comparison with clozapine and haloperidol. J Pharmacol Exp Ther 1999;288:1002–14.
[31] Mirescu C, Peters JD, Gould E. Early life experience alters response of adult neurogenesis to stress. Nat Neurosci 2004;7:841–6.
[32] Miyamoto Y, Yamada K, Noda Y, Mori H, Mishina M, Nabeshima T. Lower sensitivity to stress and altered monoaminergic neuronal function in mice lacking the NMDA receptor epsilon 4 subunit. J Neurosci 2002;22:2335–42.
[33] Muchimapura S, Mason R, Marsden CA. Effect of isolation rearing on pre- and post-synaptic serotonergic function in the rat dorsal hippocampus. Synapse 2003;47:209–17.
[34] Murphy DA, Pelham WE, Lang AR. Aggression in boys with attention deficit-hyperactivity disorder: methylphenidate effects on naturalistically observed aggression, response to provocation, and social information processing. J Abnorm Child Psychol 1992;20:451–66.
[35] Nagai T, Takuma K, Kamei H, Ito Y, Nakamichi N, Ibi D, et al. Dopamine D1 receptors regulate protein synthesis-dependent long-term recognition memory via extracellular signal-regulated kinase 1/2 in the prefrontal cortex. Learn Mem 2007;14:117–25.
[36] Nelson RJ, Trainor BC. Neural mechanisms of aggression. Nat Rev Neurosci 2007;8:536–46.
[37] Preece MA, Dalley JW, Theobald DE, Robbins TW, Reynolds GP. Region specific changes in forebrain 5-hydroxytryptamine1A and 5-hydroxytryptamine2A receptors in isolation-reared rats: an in vitro autoradiography study. Neuroscience 2004;123:725–32.
[38] Rapoport JL, Addington AM, Frangou S, Psych MR. The neurodevelopmental model of schizophrenia: update 2005. Mol Psychiatry 2005;10:434–49.
[39] Schiller L, Jähkel M, Kretzschmar M, Brust P, Oehler J. Autoradiographic analyses of 5-HT1A and 5-HT2A receptors after social isolation in mice. Brain Res 2003;980:169–78.
[40] Seeman P, Madras B. Methylphenidate elevates resting dopamine which lowers the impulse-triggered release of dopamine: a hypothesis. Behav. Brain Res 2002;130:79–83.
[41] Silva-Gómez AB, Rojas D, Juárez I, Flores G. Decreased dendritic spine density on prefrontal cortical and hippocampal pyramidal neurons in postweaning social isolation rats. Brain Res 2003;983:128–36.
[42] Spivak B, Roitman S, Vered Y, Mester R, Graff E, Talmon Y, et al. Diminished suicidal and aggressive behavior, high plasma norepinephrine levels, and serum triglyceride levels in chronic neuroleptic-resistant schizophrenic patients maintained on clozapine. Clin Neuropharmacol 1998;21:245–50.
[43] Sunohara GA, Malone MA, Rovet J, Humphries T, Roberts W, Taylor MJ. Effect of methylphenidate on attention in children with attention deficit hyperactivity disorder (ADHD): ERP evidence. Neuropsychopharmacology 1999;21:218–28.
[44] Tremolizzo L, Doueiri MS, Dong E, Grayson DR, Davis J, Pinna G, et al. Valproate corrects the schizophrenia-like epigenetic behavioral modifications induced by methionine in mice. Biol Psychiatry 2005;57:500–9.
[45] Unis AS, Cook EH, Vincent JG, Gjerde DK, Perry BD, Mason C, et al. Platelet serotonin measures in adolescents with conduct disorder. Biol Psychiatry 1997;42:553–9.
[46] Varty GB, Marsden CA, Higgins GA. Reduced synaptophysin immunoreactivity in the dentate gyrus of prepulse inhibition-impaired isolation-reared rats. Brain Res 1999;824:197–203.
[47] Võikar V, Polus A, Vasar E, Rauvala H. Long-term individual housing in C57BL/6J and DBA/2 mice: assessment of behavioral consequences. Genes Brain Behav 2005;4:240–52.

[48] Wei XY, Yang JY, Dong YX, Wu CF. Anxiolytic-like effects of oleamide in group-housed and socially isolated mice. Prog Neuropsychopharmacol Biol Psychiatry 2007;31:1189–95.
[49] Wilkinson LS, Killcross SS, Humby T, Hall FS, Geyer MA, Robbins TW. Social isolation in the rat produces developmentally specific deficits in prepulse inhibition of the acoustic startle response without disrupting latent inhibition. Neuropsychopharmacology 1994;10:61–72.
[50] Wongwitdecha N, Marsden CA. Social isolation increases aggressive behaviour and alters the effects of diazepam in the rat social interaction test. Behav Brain Res 1996;75:27–32.
[51] Wright IK, Upton N, Marsden CA. Resocialisation of isolation-reared rats does not alter their anxiogenic profile on the elevated X-maze model of anxiety. Physiol Behav 1991;50:1129–32.

Behavioural Brain Research 206 (2010) 32–37

Contents lists available at ScienceDirect

Behavioural Brain Research

journal homepage: www.elsevier.com/locate/bbr

Research report

Combined effect of neonatal immune activation and mutant DISC1 on phenotypic changes in adulthood

Daisuke Ibi[a,1], Taku Nagai[a,1], Hiroyuki Koike[a,b], Yuko Kitahara[a], Hiroyuki Mizoguchi[c], Minae Niwa[d,e], Hanna Jaaro-Peled[f], Atsumi Nitta[a], Yukio Yoneda[b], Toshitaka Nabeshima[d], Akira Sawa[f], Kiyofumi Yamada[a,g,*]

[a] *Department of Neuropsychopharmacology and Hospital Pharmacy, Nagoya University Graduate School of Medicine, Nagoya 466–8560, Japan*
[b] *Laboratory of Molecular Pharmacology, Graduate School of Natural Science and Technology, Kanazawa University, Kanazawa 920-1192, Japan*
[c] *Futuristic Environmental Simulation Center, Research Institute of Environmental Medicine, Nagoya University, Nagoya 464-8601, Japan*
[d] *Department of Chemical Pharmacology, Graduate School of Pharmaceutical Sciences, Meijo University, Nagoya 468-8503, Japan*
[e] *Department of Psychiatry, Nagoya University Graduate School of Medicine, Nagoya 466–8560, Japan*
[f] *Departments of Psychiatry and Behavioral Sciences, Johns Hopkins University School of Medicine, Baltimore, MD 21287, USA*
[g] *JST, CREST, Japan*

ARTICLE INFO

Article history:
Received 20 June 2009
Received in revised form 18 August 2009
Accepted 24 August 2009
Available online 28 August 2009

Keywords:
Schizophrenia
Gene–environment interaction
Viral infection
Polyl:C
Susceptibility gene
DISC1
Transgenic mice

ABSTRACT

Gene–environment interaction may play a role in the etiology of schizophrenia. Transgenic mice expressing dominant-negative DISC1 (DN-DISC1 mice) show some histological and behavioral endophenotypes relevant to schizophrenia. Viral infection during neurodevelopment provides a major environmental risk for schizophrenia. Neonatal injection of polyriboinosinic-polyribocytidylic acid (polyI:C), which mimics innate immune responses elicited by viral infection, leads to schizophrenia-like behavioral alteration in mice after puberty. To study how gene-environmental interaction during neurodevelopment results in phenotypic changes in adulthood, we treated DN-DISC1 mice or wild-type littermates with injection of polyI:C during the neonatal stage, according to the published method, respectively, and the behavioral and histological phenotypes were examined in adulthood. We demonstrated that neonatal polyI:C treatment in DN-DISC1 mice resulted in the deficits of short-term, object recognition, and hippocampus-dependent fear memories after puberty, although polyI:C treatment by itself had smaller influences on wild-type mice. Furthermore, polyI:C-treated DN-DISC1 mice exhibited signs of impairment of social recognition and interaction, and augmented susceptibility to MK-801-induced hyperactivity as compared with vehicle-treated wild-type mice. Of most importance, additive effects of polyI:C and DN-DISC1 were observed by a marked decrease in parvalbumin-positive interneurons in the medial prefrontal cortex. These results suggest that combined effect of neonatal polyI:C treatment and DN-DISC1 affects some behavioral and histological phenotypes in adulthood.

1. Introduction

Genetic susceptibility factors for schizophrenia have recently become available; these include *neuregulin-1*, *dysbindin*, and *disrupted-in-schizophrenia 1* (*DISC1*) [9]. Maternal viral infection in the first and second trimesters of pregnancy in humans increases the risk of schizophrenia in young adulthood [3,4,22]. Furthermore, the possible interaction between environmental and genetic susceptibility factors, especially during neurodevelopment, is proposed as a promising disease etiology of schizophrenia [5,14].

Here we study a possible interaction of genetic and environmental factors by injecting a synthetic double-stranded RNA, polyriboinosinic-polyribocytidylic acid (polyI:C) into transgenic mice that express a dominant-negative form of DISC1 (DN-DISC1). We chose DISC1 as a genetic factor on which to focus, because its role during neurodevelopment is well characterized [6,13]. DN-DISC1 mice show some behavioral (sensorimotor gating deficits, depression-like behavior and hyperactivity) and histological (enlarged lateral ventricles and reduction in the immunoreactivity of parvalbumin in the cortex) endophenotypes relevant to schizophrenia [10]. PolyI:C is a toll-like receptor 3 ligand that induces a strong innate immune response, and has been used to mimic viral infection during neurodevelopment [15,23].

* Corresponding author at: Department of Neuropsychopharmacology and Hospital Pharmacy, Nagoya University Graduate School of Medicine, Nagoya 466–8560, Japan. Tel.: +81 52 744 2674; fax: +81 52 744 2682.
E-mail address: kyamada@med.nagoya-u.ac.jp (K. Yamada).
[1] These authors contributed equally to the work.

0166-4328/$ – see front matter © 2009 Elsevier B.V. All rights reserved.
doi:10.1016/j.bbr.2009.08.027